

Time Resolution Studies of 4H-SiC LGADs for Fast Timing Applications

Tao Yang¹, Ben Sekely², Yashas Satapathy², Greg Allion², Gil Atar², Philip Barletta², Carl Haber¹, Steve Holland¹, John Muth², Spyridon Pavlidis², Stefania Stucci³, Abraham Tishelman-Charny³

¹ Lawrence Berkeley National Laboratory

² North Carolina State University

³ Brookhaven National Laboratory

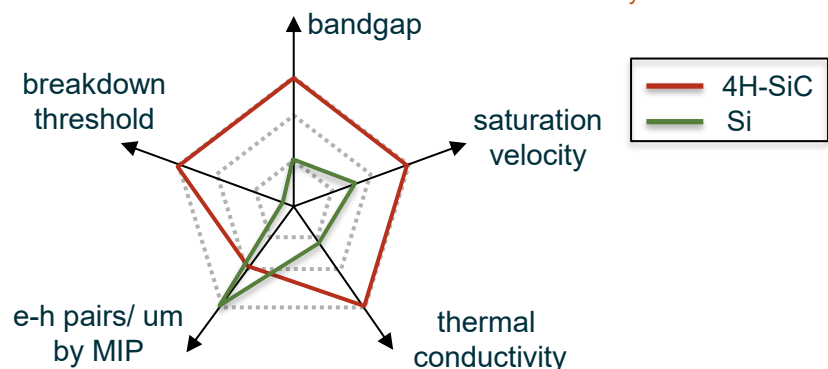
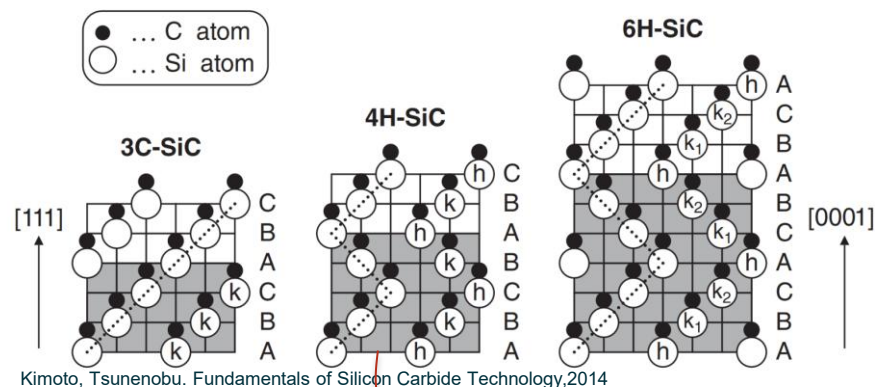
Coordinating Panel for Advanced Detectors (CPAD) Workshop, 2025, Pennsylvania

2025-10-09

Silicon Carbide for Charged Particle Detection

As a wide-band semiconductor material, among many silicon carbide (SiC) polymorphs, 4H-SiC has potential applications in radiation detection, especially **fast time detection** and **high temperature environment**.

Schematic structures of popular SiC polytypes: 3C, 4H and 6H



The parameters of Si and 4H-SiC

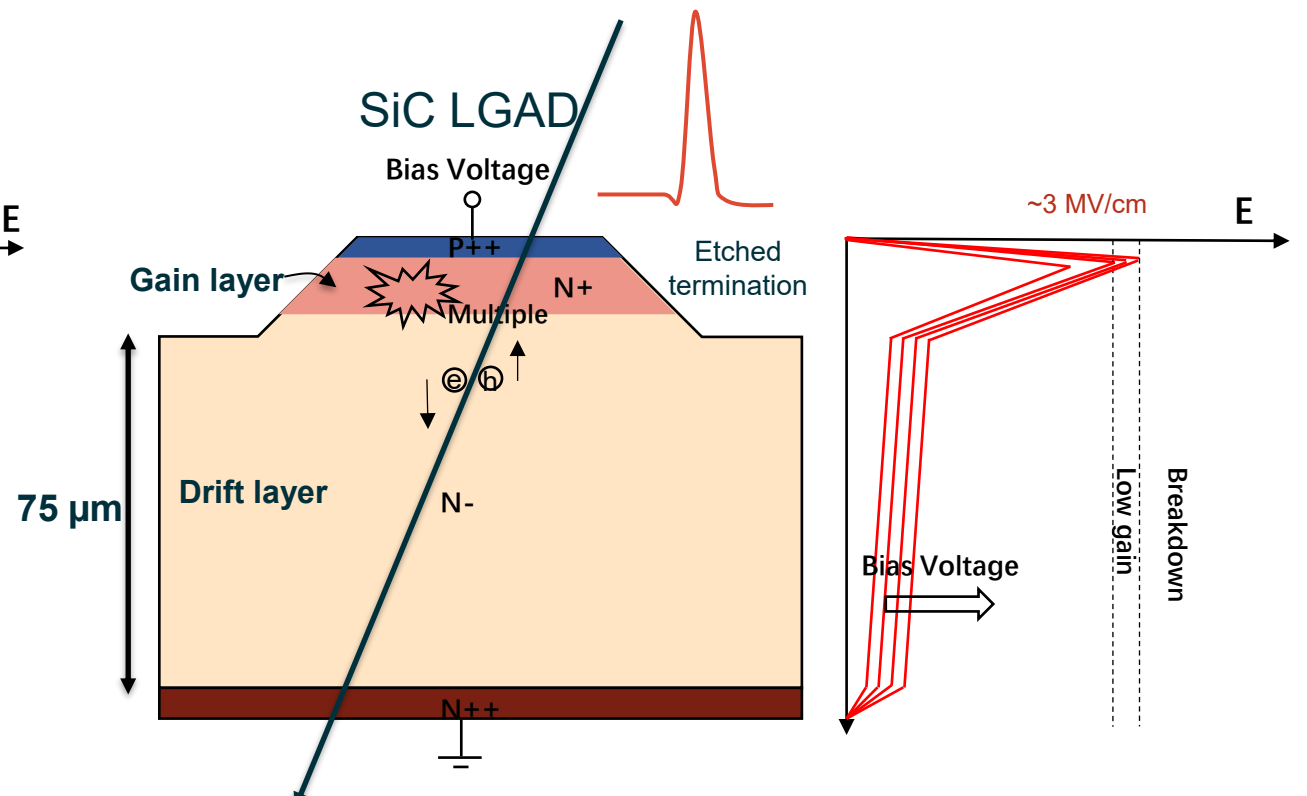
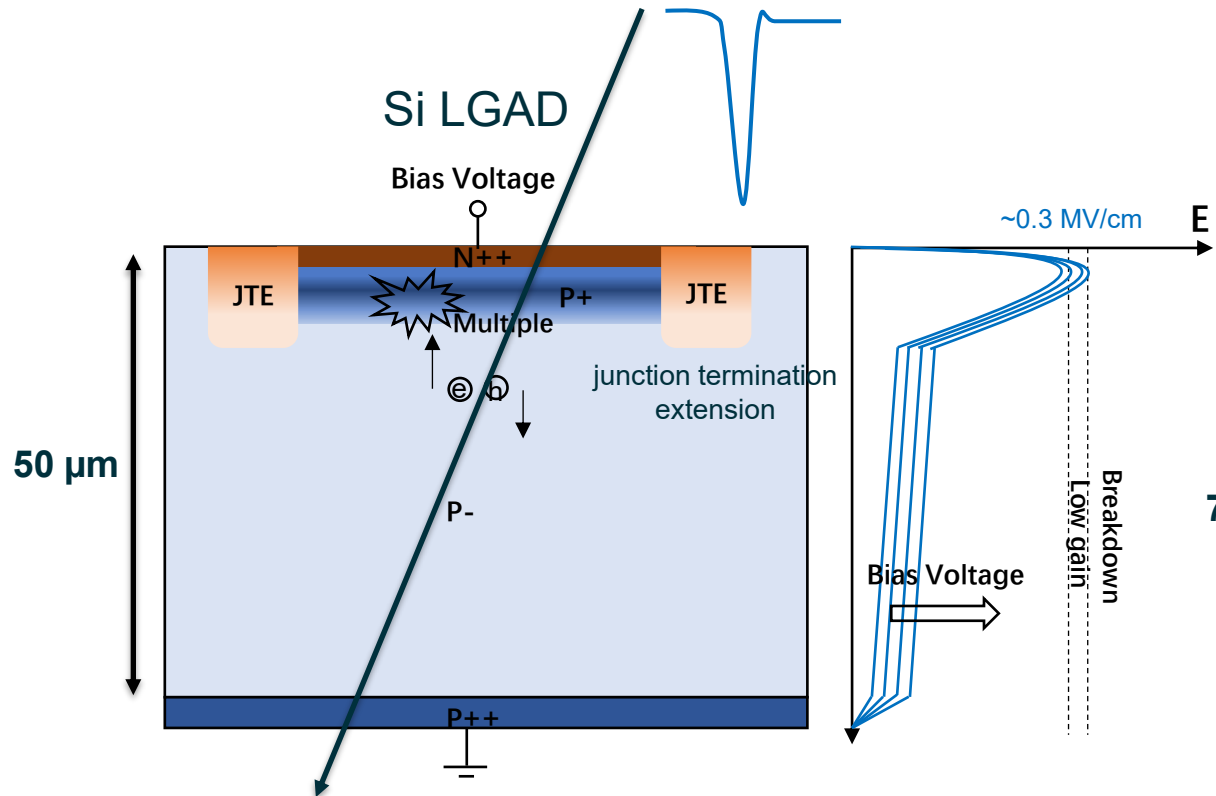
Parameters	Si	4H-SiC
Band gap[eV]	1.12	3.26
Relative permittivity	11.7	9.76
Thermal conductivity[W/K·cm]	1.5	4.9
Average ionization energy [eV/e-h pair]	3.6	5-9
Average e-h pairs for MIP [μm^{-1}]	~78	~55
Breakdown Threshold [MV/cm]	~0.3	~2.0
Atom displacement energy [eV]	13-15	30-40
Fano factor	0.11-0.13	0.04-0.12
Electron mobility [cm^2/Vs]	1450	800
Hole mobility [cm^2/Vs]	450	115
Electron saturation velocity [cm/s]	1×10^7	2×10^7
Hole saturation velocity [cm/s]	0.6×10^7	1.8×10^7



Silicon Carbide Low Gain Avalanche Detector (SiC LGAD)

- 50 μm P-type ($\sim 1\text{e}13 \text{ cm}^{-3}$) drift layer
- Primary electrons multiplication.
- Ion implantation for gain layer and JTE
- Electric field: $\sim 0.3 \text{ MV/cm}$
- Gain layer doping: $\sim 1\text{e}16 \text{ cm}^{-3}$

- 75 μm N-type drift layer ($\sim 2\text{e}14 \text{ cm}^{-3}$)
- Primary holes multiplication.
- Epitaxial stack with etched termination (or ion implantation)
- Electric field: $\sim 3 \text{ MV/cm}$
- Gain layer doping: $> 2\text{e}17 \text{ cm}^{-3}$



The Design & Fabrication of 4H-SiC LGAD by LBNL and NCSU

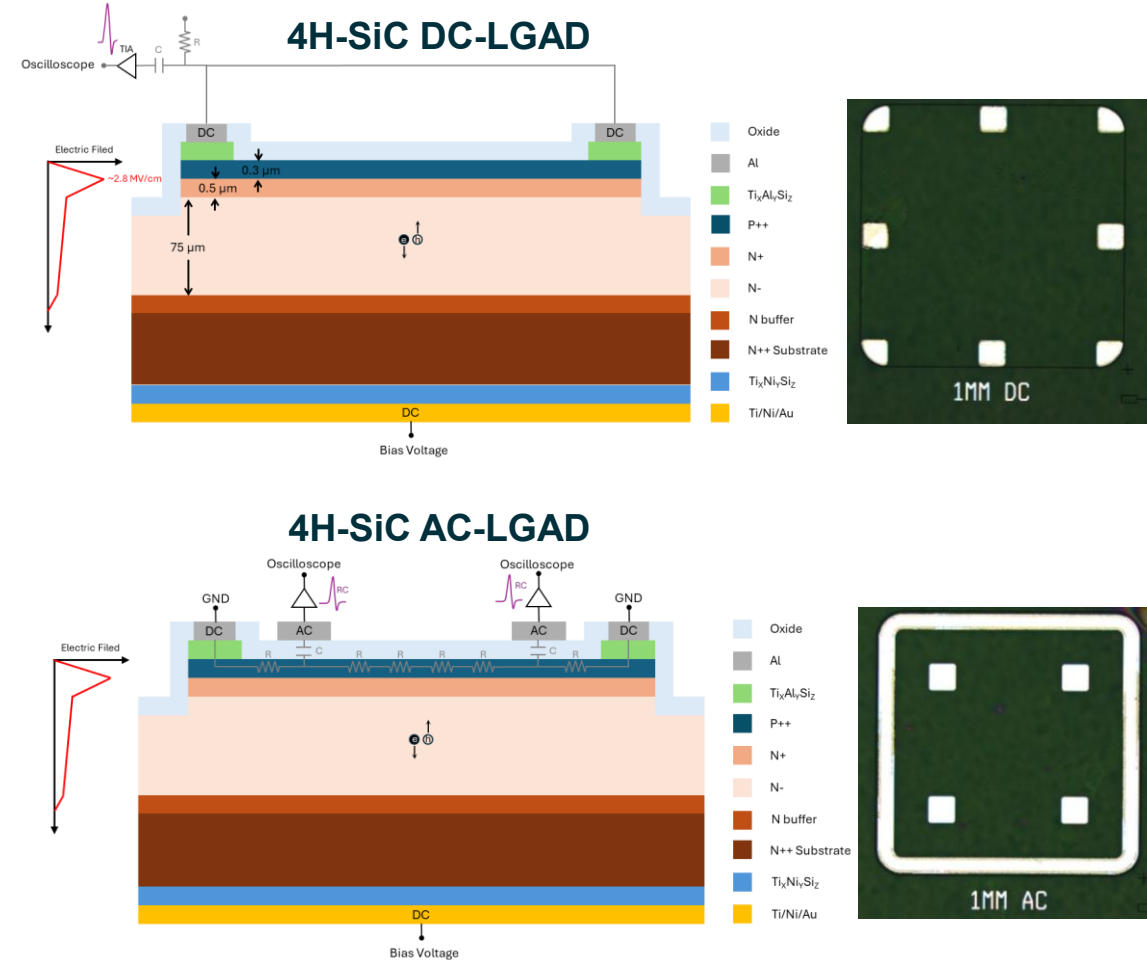
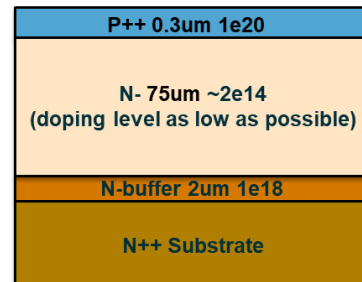
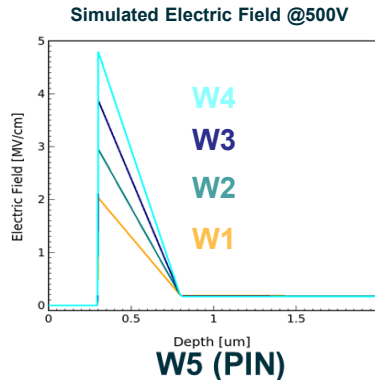
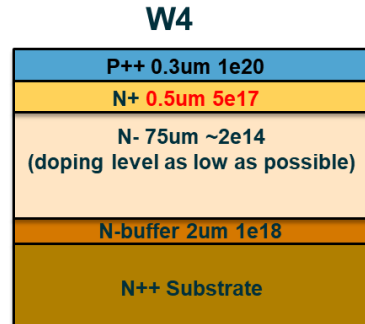
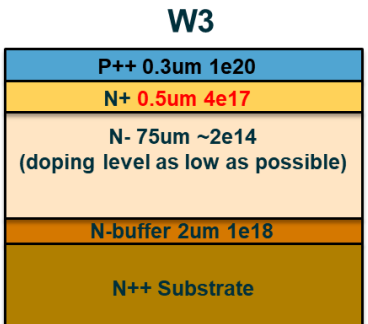
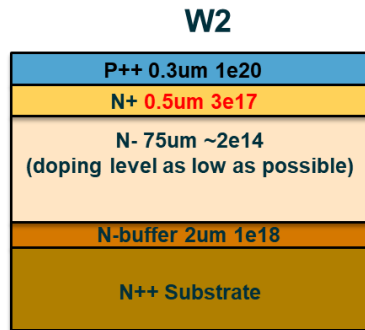
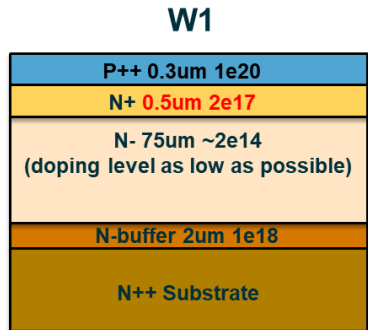
Based on 6-inch 4H-SiC wafers with custom epitaxial stacks

- 0.5 μm Gain layer with doping concentration from $2e17 \text{ cm}^{-3}$ to $5e17 \text{ cm}^{-3}$, which target the electric field between 2 MV/cm to 5 MV/cm .
- Etched-Termination isolates the segmented devices.

Sekely, B.J., et. al. Fabrication of 4H-SiC Low Gain Avalanche Detectors (LGADs). [10.4028/p-0t5ifB](https://arxiv.org/abs/10.4028/p-0t5ifB)

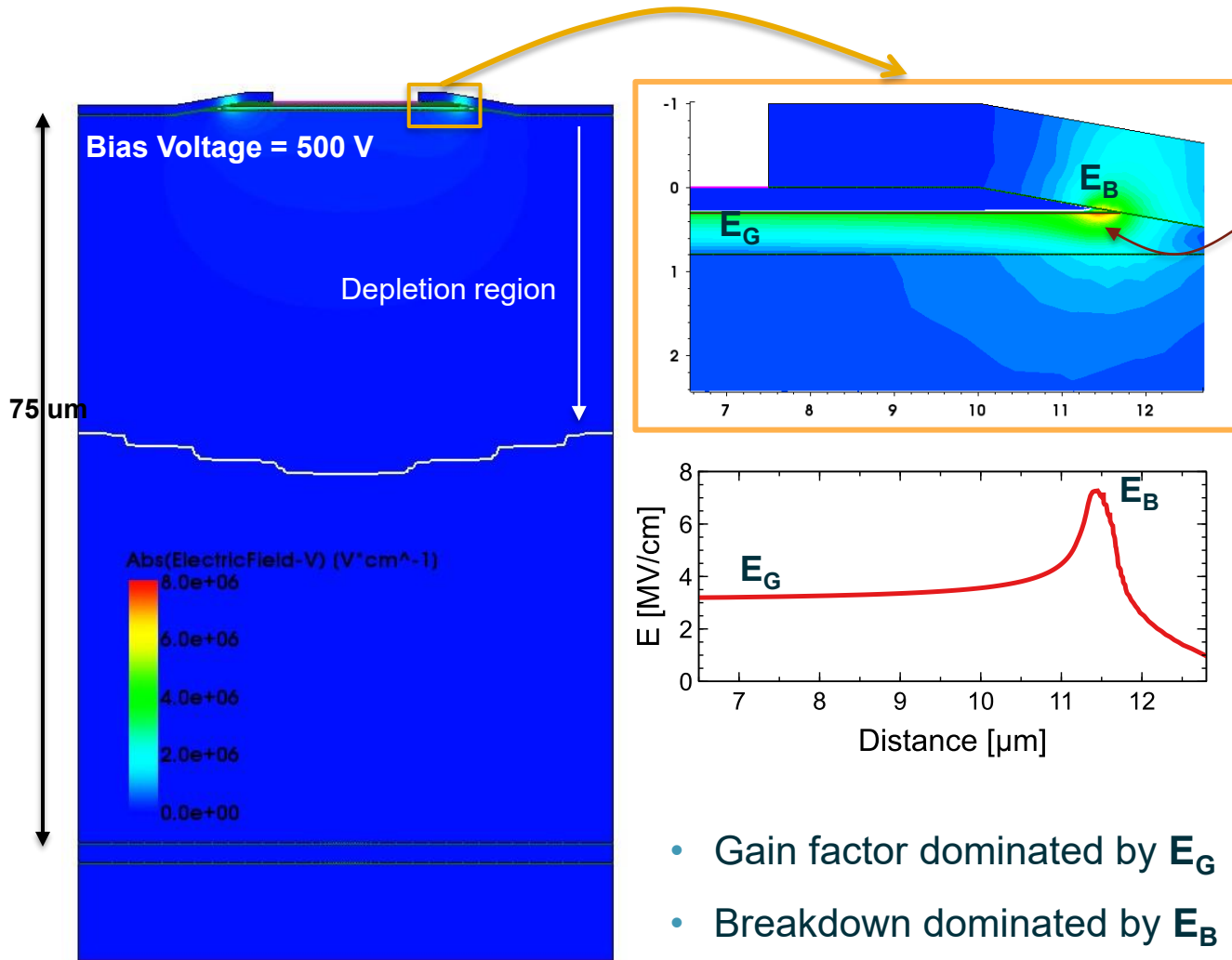
Yang, T., et. al. Characterization of 4H-SiC Low Gain Avalanche Detectors (LGADs). [10.1016/j.nima.2025.170873](https://arxiv.org/abs/10.1016/j.nima.2025.170873)

Custom Epitaxial Wafers



Issue of 4H-SiC LGAD with Bevel-Etched Termination

The bevel-etched 4H-SiC LGADs currently have to adopt a **negative bevel-etched angle**, which increases the junction electric field on the surface of bevel, leading to a reduction in the breakdown voltage.



- 1) The electric field peak E_B appears close to the bevel surface.
- 2) High bias voltage (>1000 V) should be applied to deplete N-type drift layer($d=75\mu\text{m}$, $N_{\text{eff}}=2\text{e}14 \text{ cm}^{-3}$)

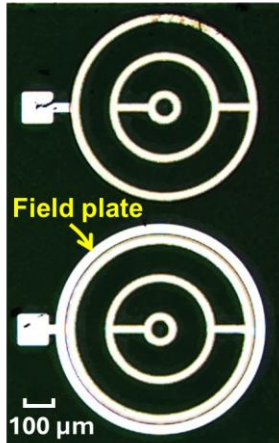
$$V_{\text{dep}} = \frac{q|N_{\text{eff}}|d^2}{2\epsilon\epsilon_0}$$

- 3) The E_B exceeds the breakdown threshold easily when the bias voltage increase, that caused the device **breakdown before full depletion (<1000 V)**.

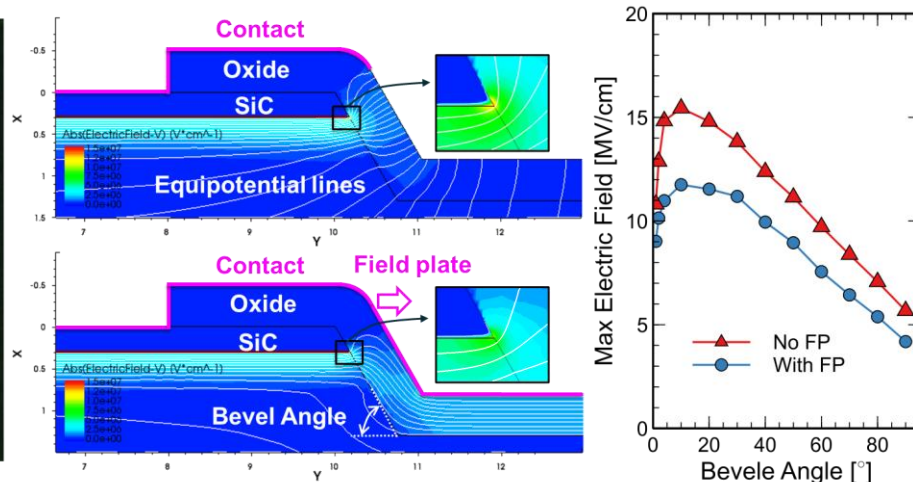
- Gain factor dominated by E_G
- Breakdown dominated by E_B

The Effects of Field Plate

Device Sample

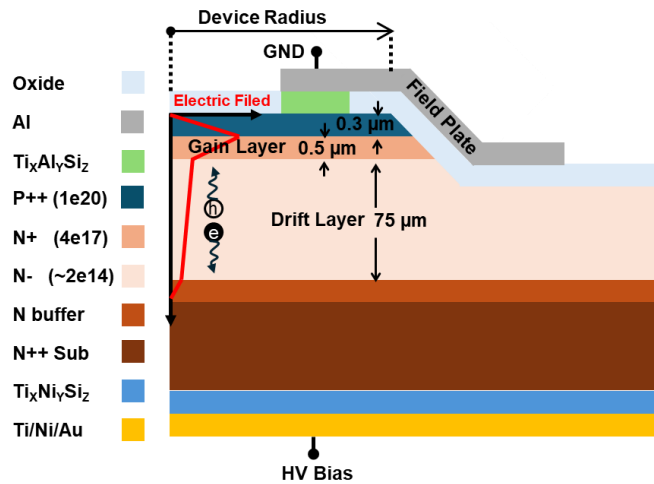


Simulation

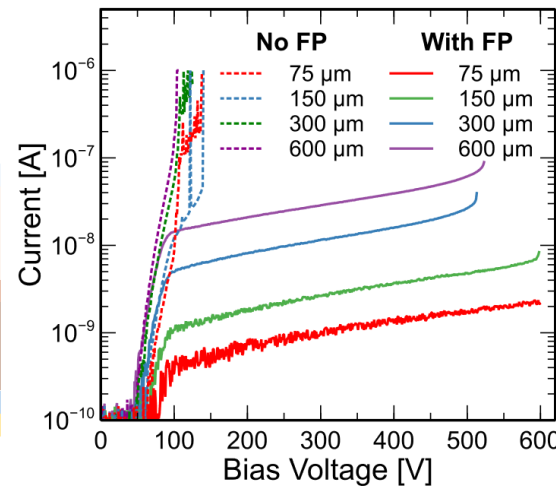


Higher breakdown voltage by lower electric field with field plate.

- The equipotential lines are reshaped to parallel with the surface by the extended field plate. Then the electric field is suppressed.
- Observed higher breakdown voltage for the devices with field plate.



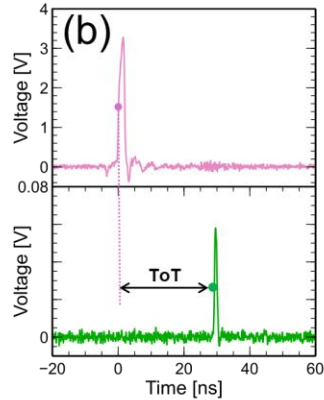
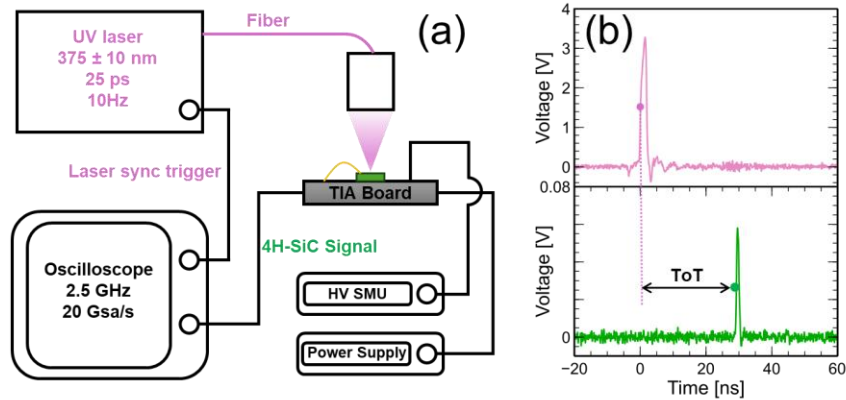
I-V Measurement



Field plate can effectively increase breakdown voltage.

Time Resolution of SiC LGAD by UV-TCT

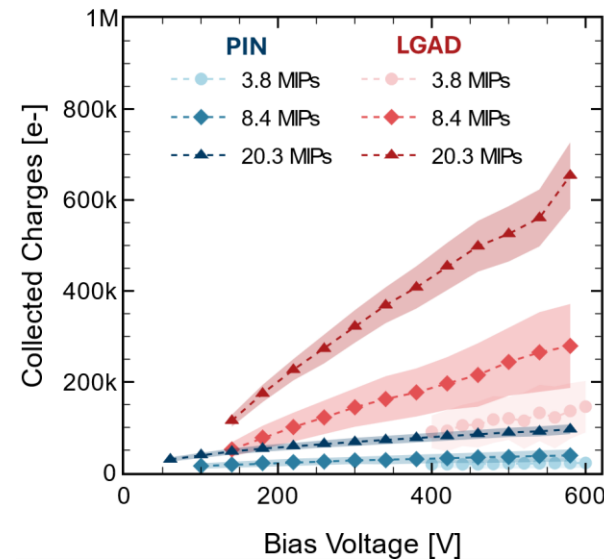
UV-TCT Setup for SiC DC-LGAD / PIN



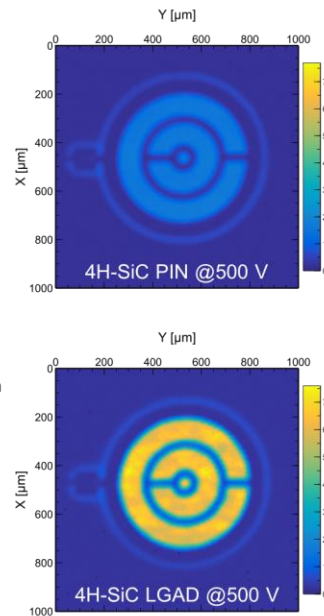
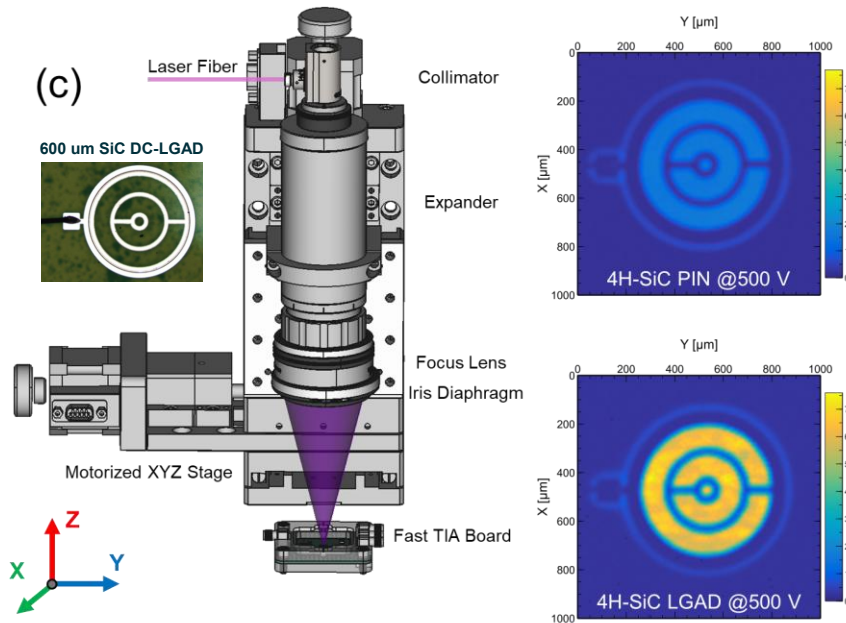
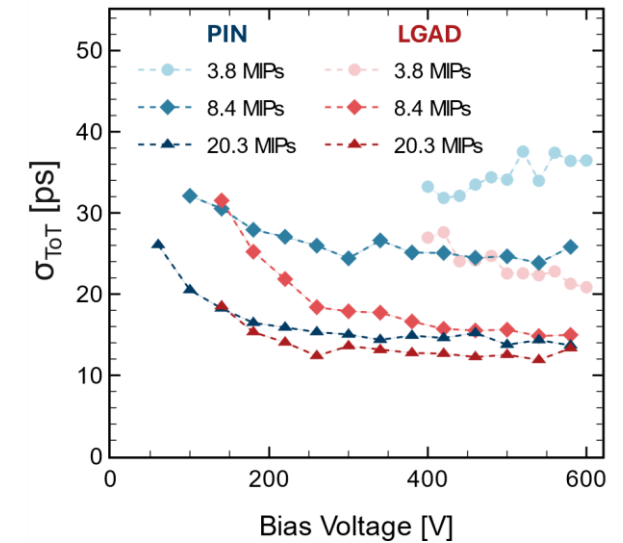
- The 4H-SiC LGAD possesses good time resolution **better than 35 ps** by UV-TCT, significantly outperforming the 4H-SiC PIN in measuring single MIP signals.

Yang, T., et. al. Ultra-Fast 4H-SiC LGAD With Etched Termination and Field Plate. [10.1109/LED.2025.3548509](https://doi.org/10.1109/LED.2025.3548509)

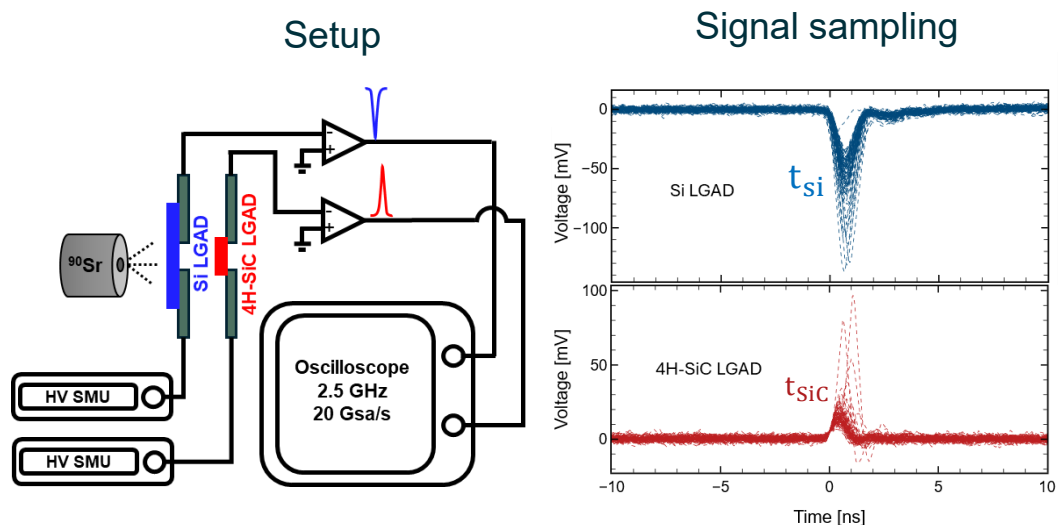
Charge Collection



Time Resolution



^{90}Sr Source Test for SiC LGAD

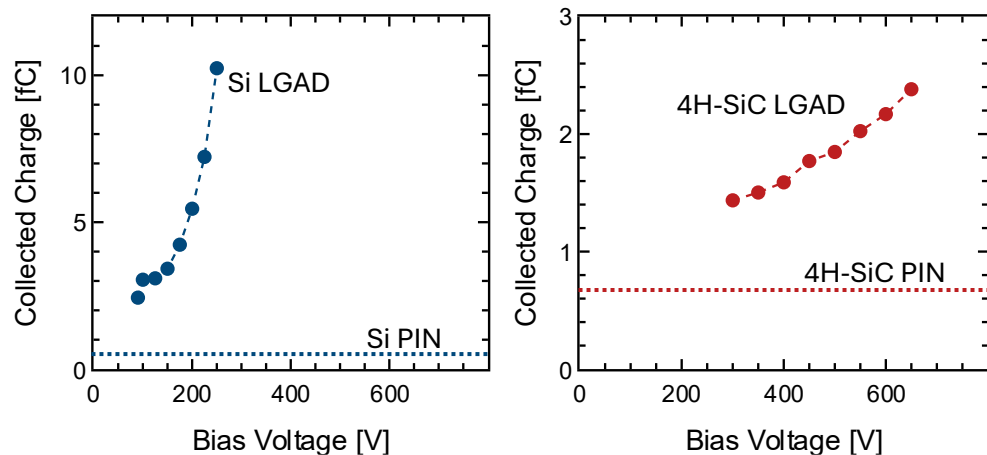


- A 50 μm thick Si LGAD with a gain of 10-20 from BNL is used as the timing reference.
- High-speed readout boards, each equipped with a 2 GHz bandwidth transimpedance amplifier.
- The signal polarity of Si LGAD and SiC LGAD is opposite.

P-type Si LGAD: 10~20 gain

N-type SiC LGAD: 2~3 gain

Charge Collection

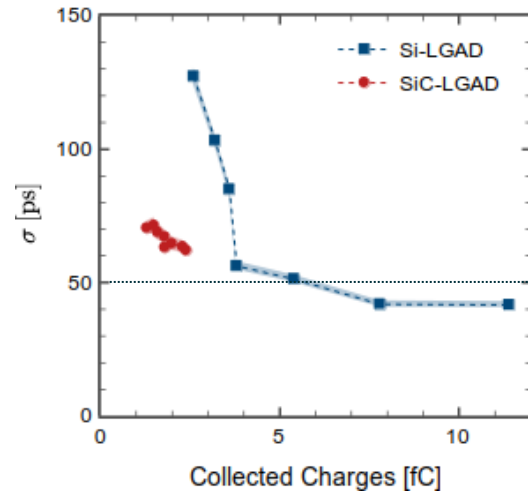
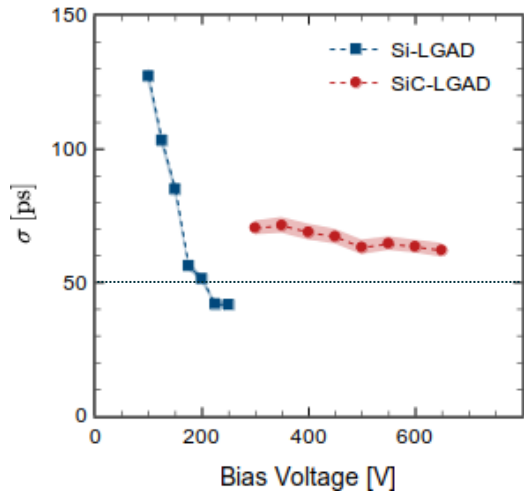


- Using the constant fraction discrimination (CFD) technique, the timing points at the same fraction of the pulse amplitude are extracted

$$\text{ToT} = t_{\text{SiC}} - t_{\text{Si}}$$

Time Resolution of SiC LGAD by β Source

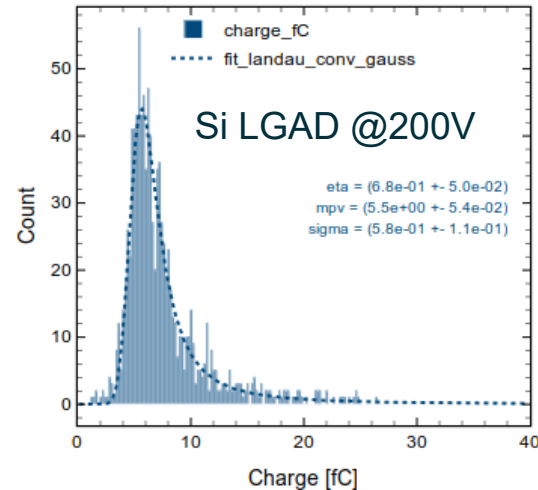
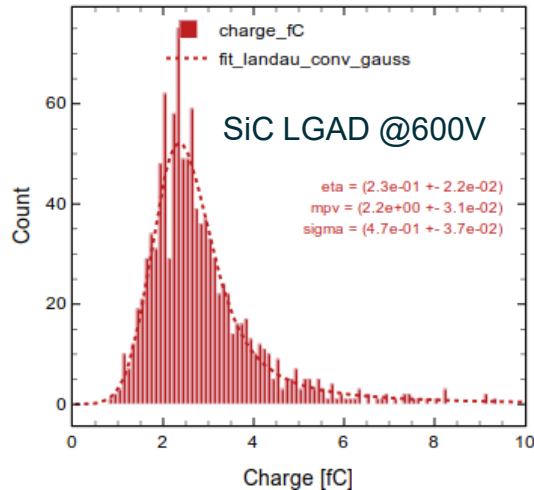
Time Resolution



$$\sigma_{\text{SiC}} = \sqrt{\sigma_{\text{TOT}}^2 - \sigma_{\text{Si}}^2}$$

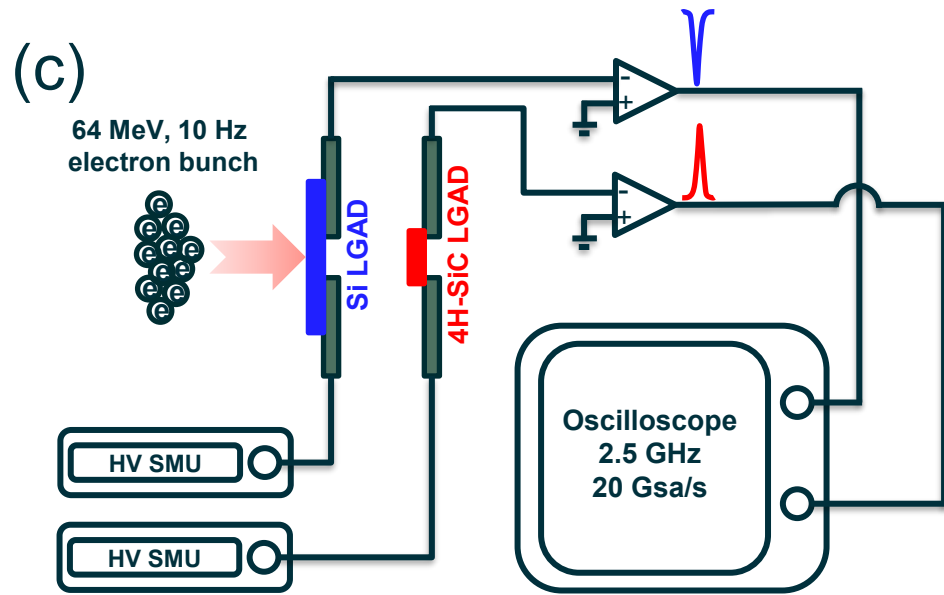
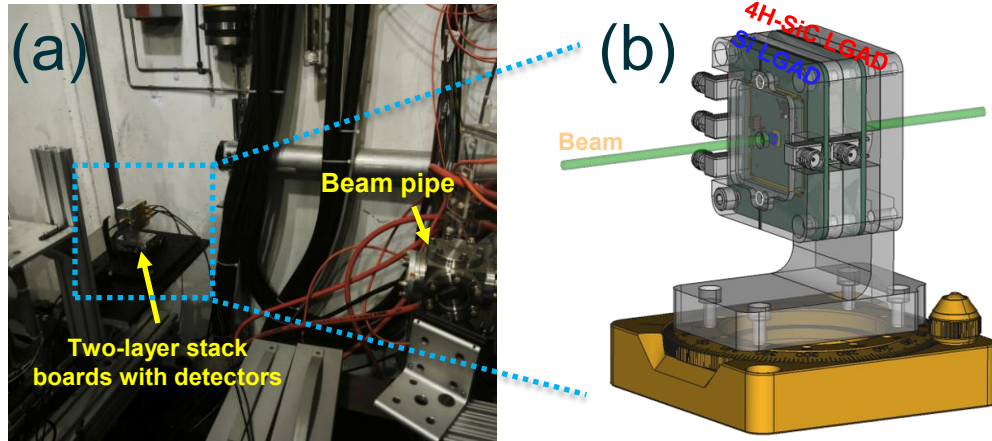
- The 4H-SiC LGADs exhibit fast signal responses, and a time resolution of **61 ps** was achieved, comparable to that of standard Si LGADs.
- The present limitation in the time resolution of 4H-SiC LGADs appears to stem from limited charge generation.
- Need to explore ways to achieve a lower doping concentration in the drift layer and increase the gain with a limited bias voltage.

Charge Distribution

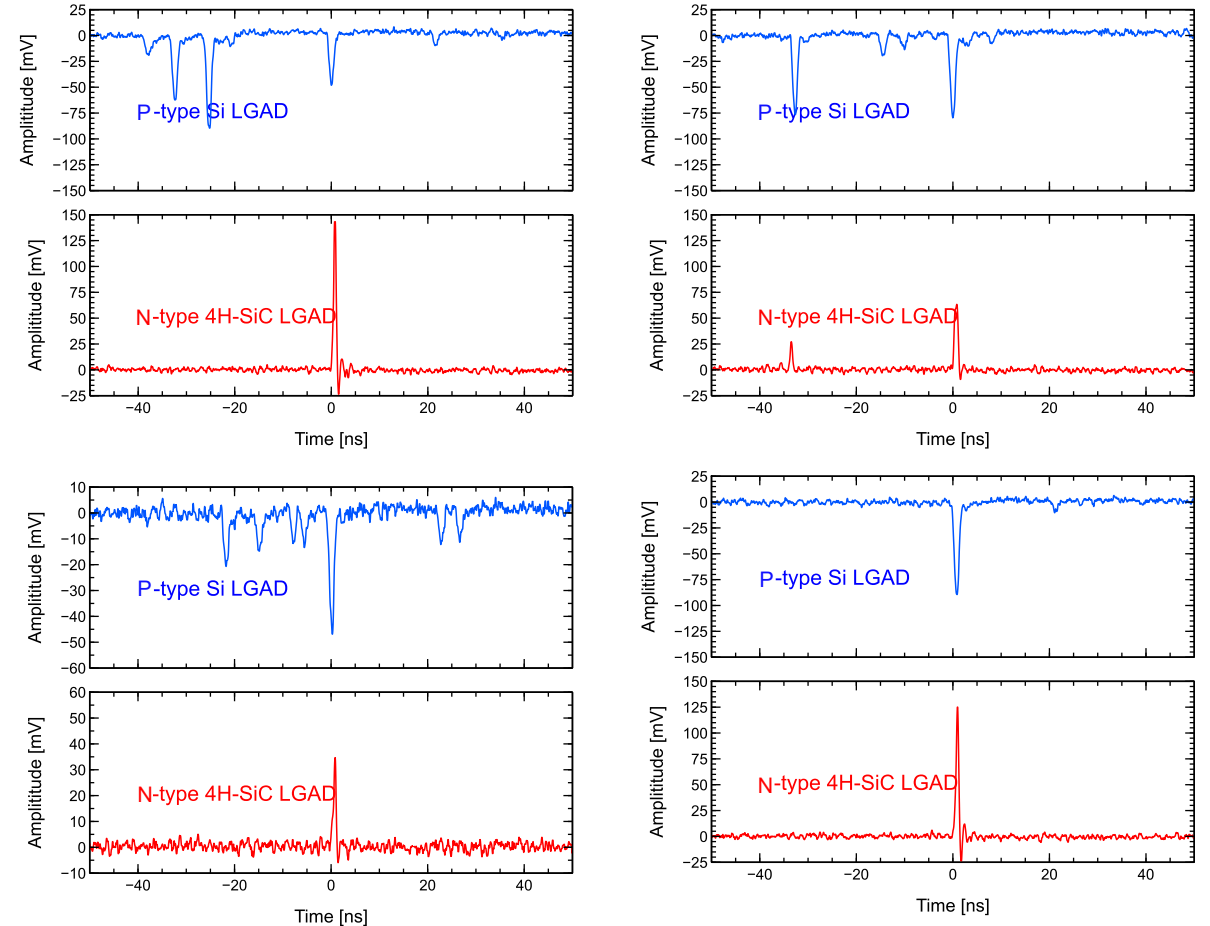


Electron Beam Test

- Beam test is by the 64 MeV electron beam in the NLCTA tunnel at SLAC.
- For comparison with SiC LGAD and time reference, a 50 μm Si LGAD with $\sigma_T < 40$ ps fabricated by BNL was used.



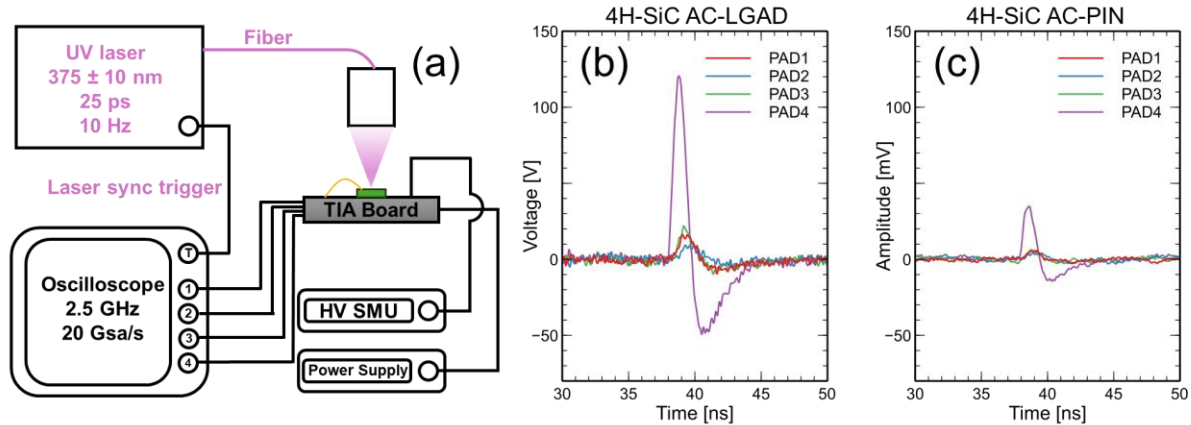
Representative signal samples



The analysis of the data are currently in progress...

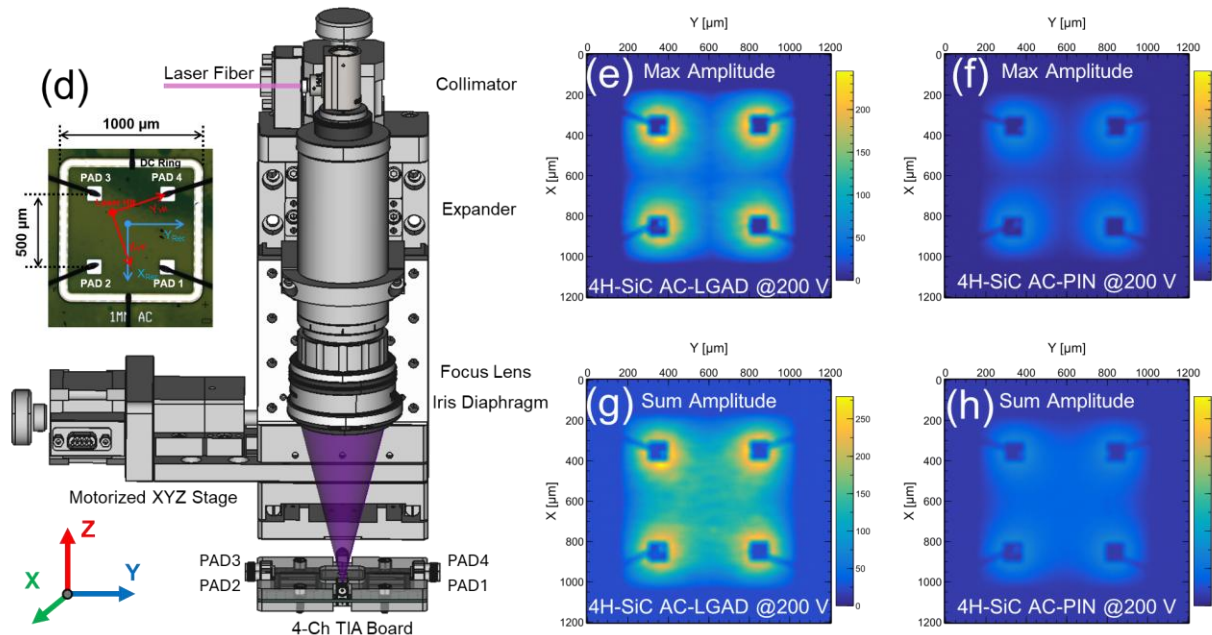
4D Tracking Application of SiC AC-LGAD

UV-TCT Setup for SiC AC-LGAD / PIN

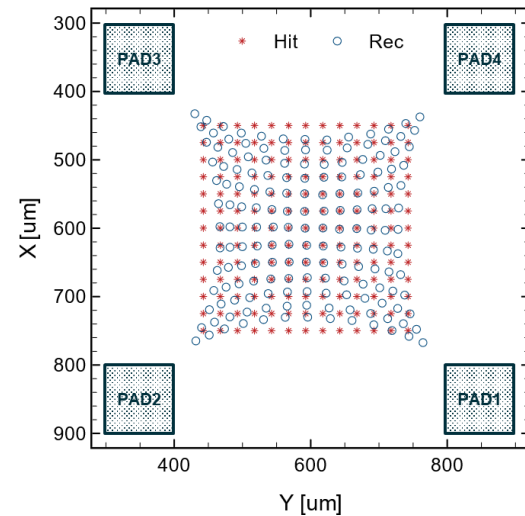


- The SiC AC-LGAD demonstrates good position resolution with $\sigma = 5.8 \mu\text{m}$ in the central region.
- The reconstructed position near the edges currently exhibits distortion due to limitations in the reconstruction algorithm (pad shape and charges leakage by DC-Ring), this issue can be addressed through **algorithm optimization** and **electrode shape optimization**.

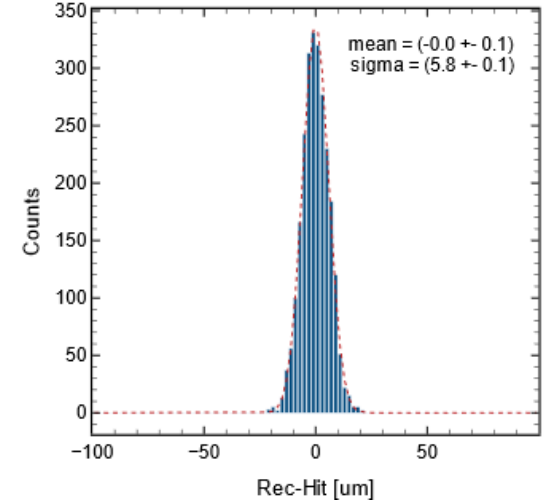
More results are currently in progress...



Rec by DPC Method

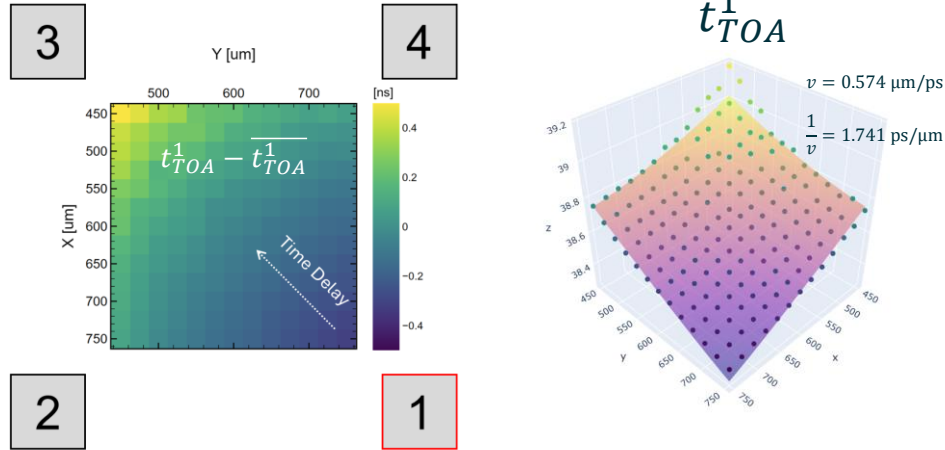


Rec - Hit



4D Tracking Application of SiC AC-LGAD

The variation in transmission distance results in corresponding time delays.

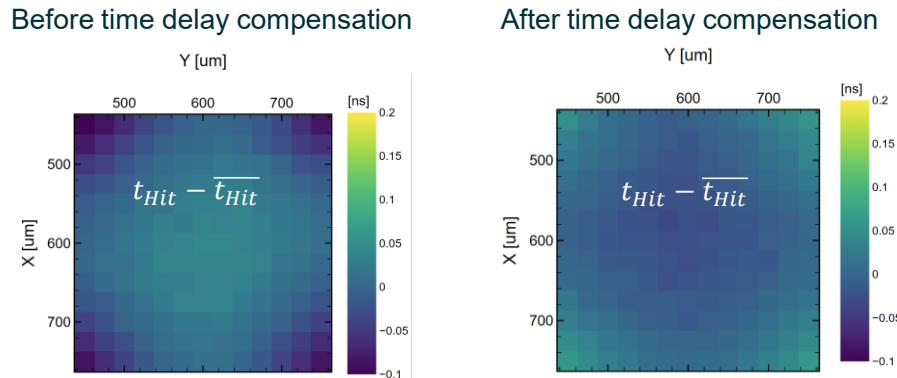


$$t_{Hit}^i = t_{ToA}^i - t_{Offset}^i - d^i/v$$

$$t_{Hit} = \frac{\sum_{i=1}^{i=4} t_{Hit}^i \times a_i}{\sum_{i=1}^{i=4} a_i}$$

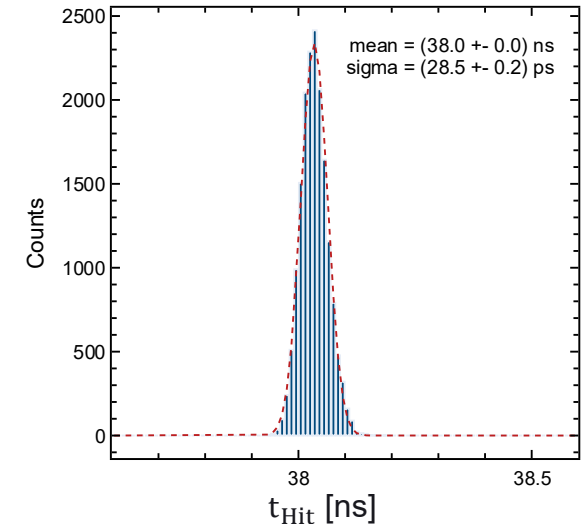
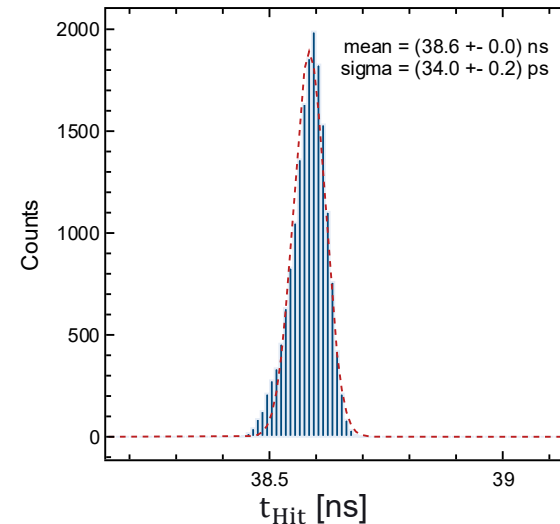
Where t_{TOA}^i is the arrival time of signal induced on the four ac pads. t_{Offset}^i is the time compensation term accounting for the different cable lengths. d^i/v is the time delay associated with the transmission distance d^i by velocity v .

Time Resolution



Before time delay compensation

After time delay compensation



Conclusion

Following two years of research and development...

- We have successfully fabricated 4H-SiC LGADs and proposed a simple and effective method to suppress the electric field and improve the breakdown voltage by introducing a **field plate**.
- The 4H-SiC LGADs demonstrate fast-timing performance in both UV-TCT and beta-source measurements, comparable to that of state-of-the-art Si LGADs.
- The current time resolution of the 4H-SiC LGADs is limited by the reduced signal charge, which arises from the lower ionization energy deposition in SiC, the relatively small internal gain, and the partially depleted drift layer.
- The beam test and the UV-TCT results of the AC-LGADs have preliminarily demonstrated the 4D tracking capability of the 4H-SiC LGADs.

Ongoing Work:

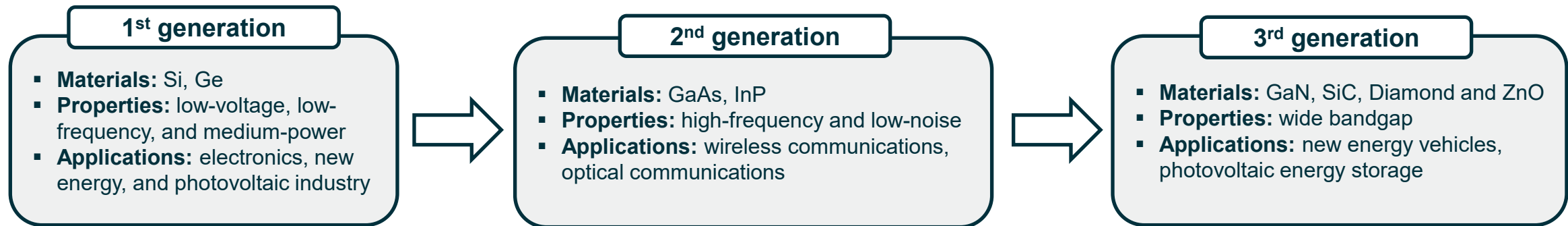
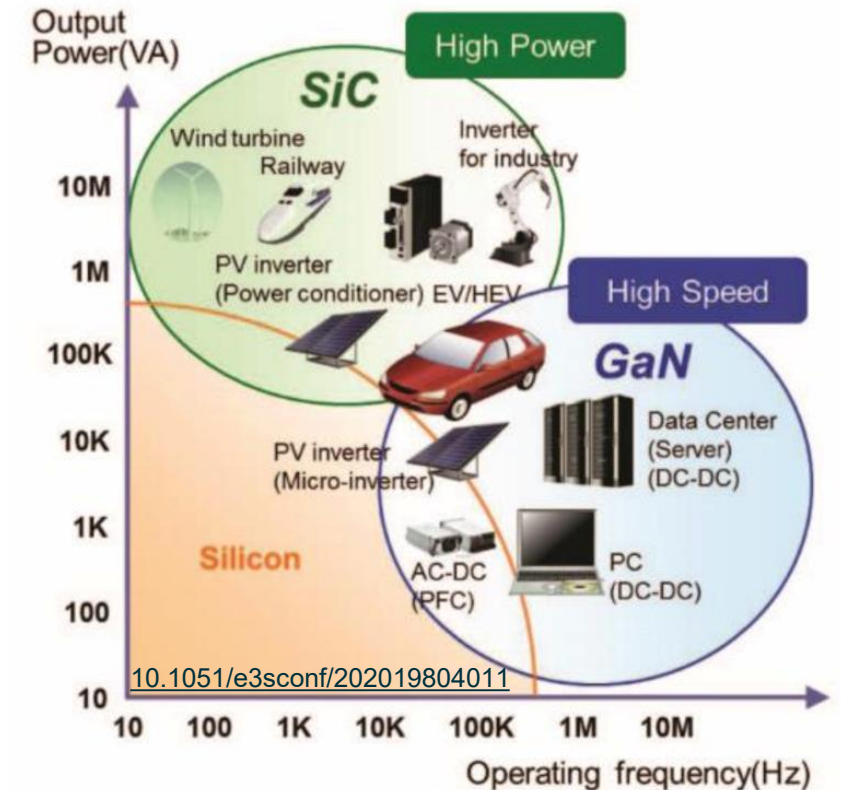
- Fabrication of 4H-SiC LGADs with higher gain
- Development of epitaxial wafers with lower drift-layer doping concentration
- 4H-SiC LGAD with Ion implantation
- Geometrical optimization of SiC AC-LGAD

Thanks for your attention

Backup

Third generation (Wide Bandgap) Semiconductors

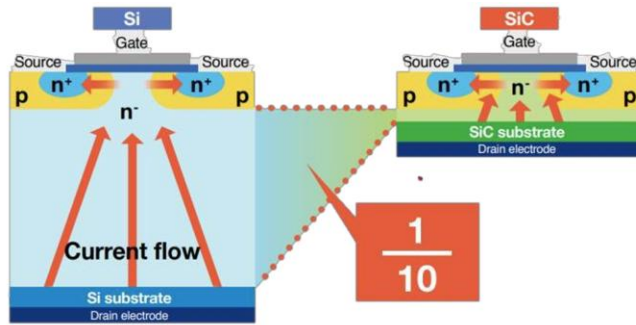
- **First generation semiconductors (indirect bandgap & narrow bandgap)** : Since 1950, semiconductor materials represented by silicon (**Si**) have replaced electron tubes, which is suitable for **low-voltage, low-frequency, and medium-power** integrated circuits.
- **Second-generation semiconductors (direct bandgap & narrow bandgap)** : Since 1990, such as gallium arsenide (**GaAs**), indium phosphide (**InP**). They are suitable for making **high-speed, high-frequency, high-power and light-emitting electronic devices**.
- **Third generation semiconductors (direct bandgap & wide bandgap)** : long history but limited by process technologies. In recent years, materials represented by gallium nitride (**GaN**) and silicon carbide (**SiC**) have attracted much attention with the development of process technologies, which are suitable for making **high temperature, high frequency and high power devices**.



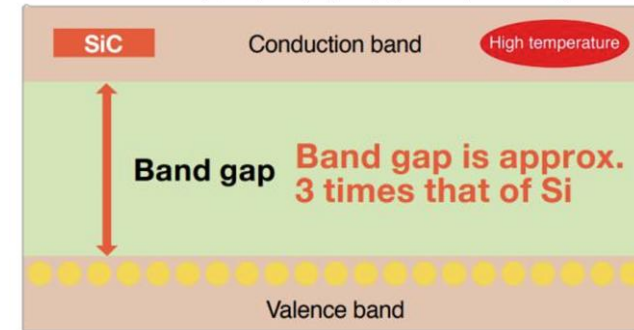
Silicon Carbide(SiC) for Integrated Circuit

Silicon Carbide is useful for power devices and high-speed switching.

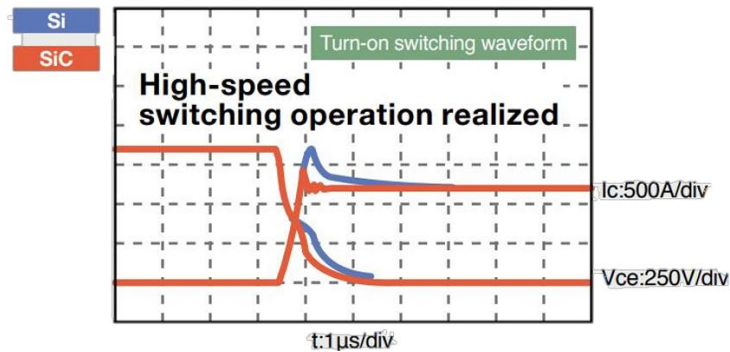
- **Low power consumption:** On-resistance of SiC device is only 1/10 of that of Si



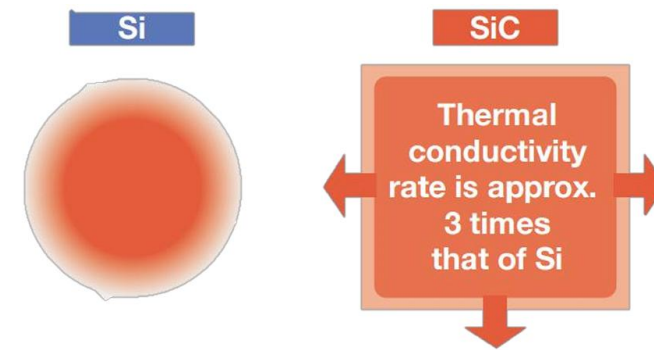
- **High temperature resistance:** SiC's bandgap is three times that of Si, preventing leakage current flow and allowing operation at high temperatures.



- **High-speed switching:** high drift velocity and small transit time



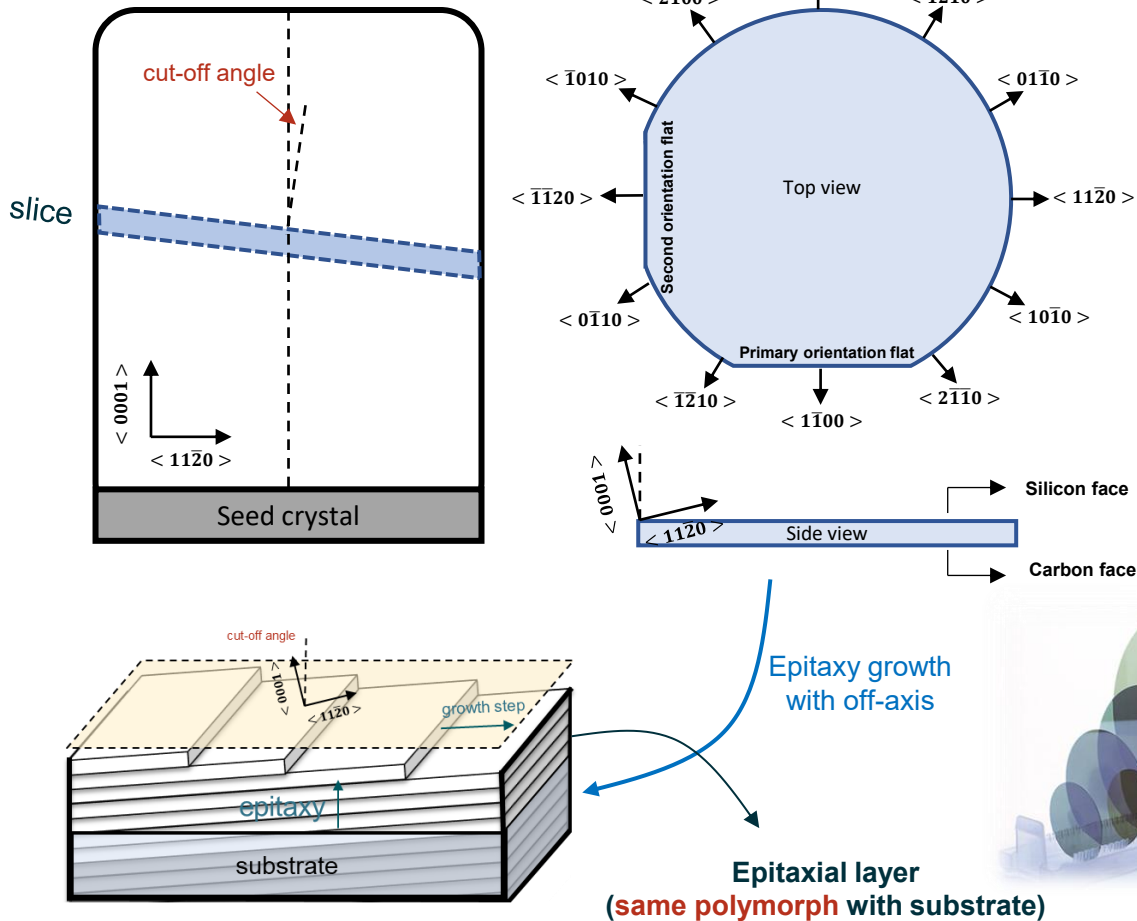
- **Heat dissipation:** the thermal conductivity of SiC is about 3 times that of Si, which dissipates heat quickly.



Epitaxial Growth of Silicon Carbide

Silicon Carbide has had a long history, but for many years was limited by crystal quality including micropipes and basal plane defects. Schottky Barrier Diodes were first made widely available in the early 2000's followed by the commercialization of high voltage MOSFETS around 2011.

SiC Wafer and Epitaxial Growth

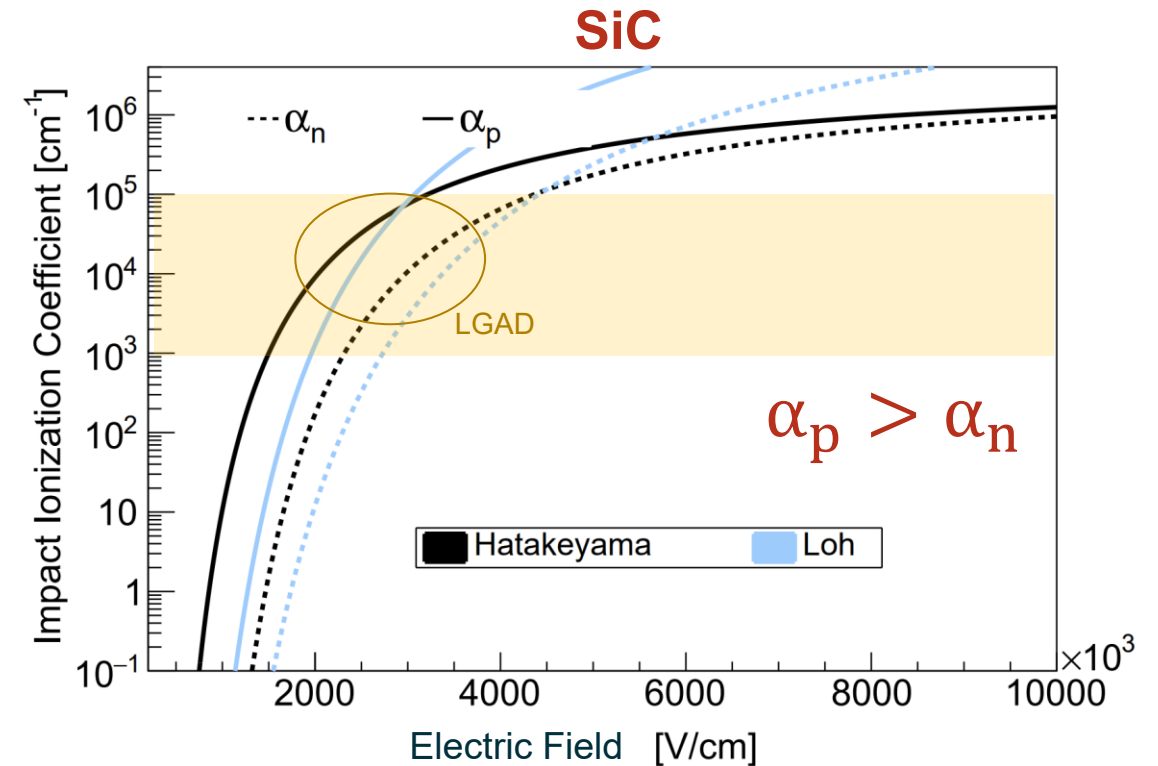
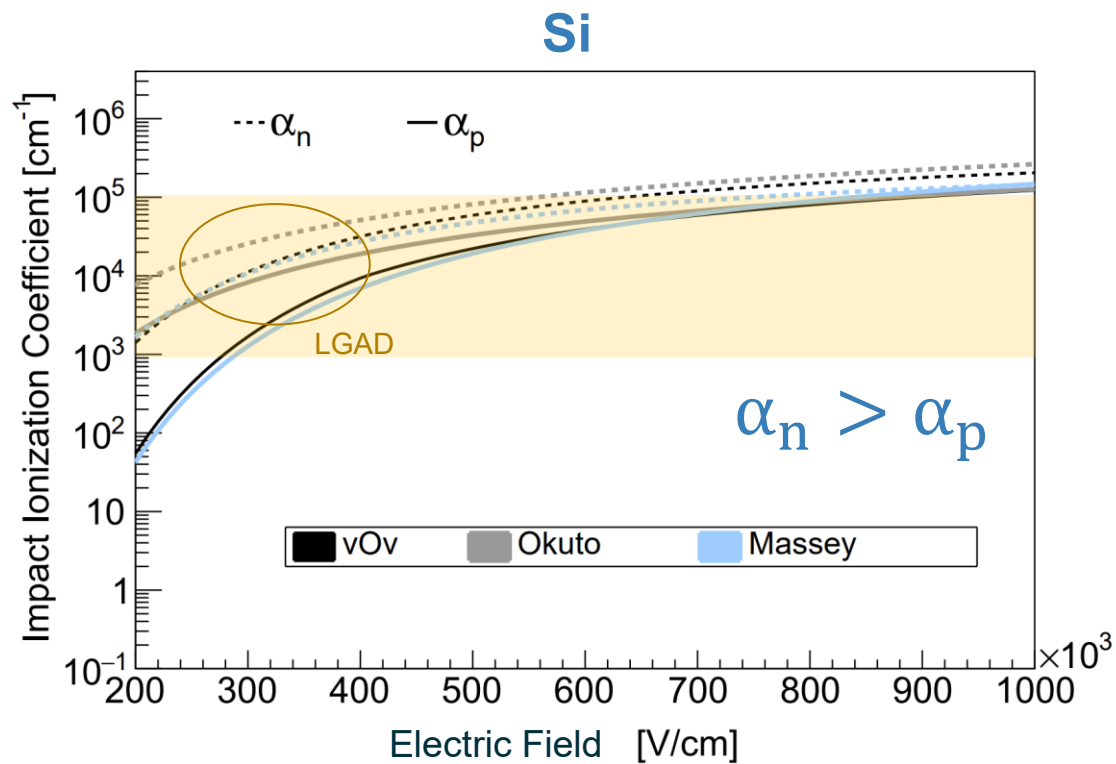


- Benefiting from **off-axis** epitaxial growth technology, which provides high purity, good doping control and uniformity, SiC became the preferred choice for power device fabrication in the mid-1990s.
- Currently there are several vendors offering SiC epitaxy and wafers, with the number of wafers produced per year growing rapidly as SiC is adopted to replace silicon in power electronics.

- wafer size: 3 / 4 / 6 / 8 inch
- epi thickness: <math>< 200 \mu\text{m}</math>
- epi doping range: $1\text{e}14 \sim 2\text{e}19 \text{ cm}^{-3}$

Impact ionization coefficient $\alpha_{Si} > \alpha_{SiC}$

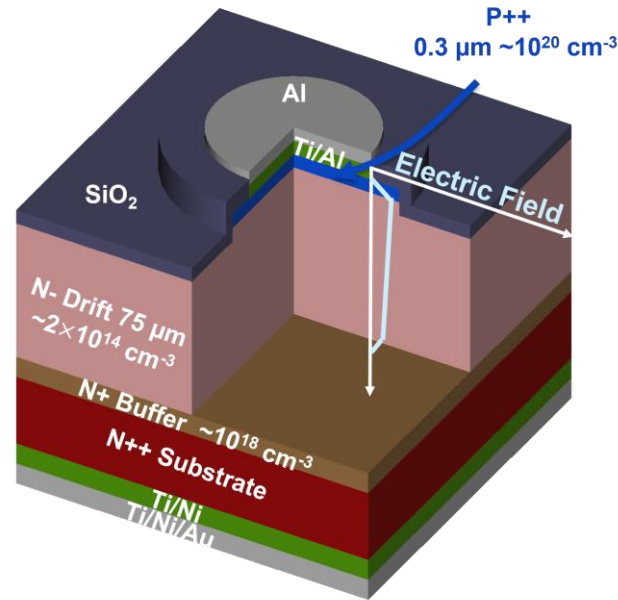
- In silicon carbide, it has smaller impact ionization coefficient than silicon at the same electric field. And the holes has larger impact ionization coefficient. Thus, the SiC LGAD should be designed with **N-type drift layer** and higher electric field (Si: ~ 0.3 MV/cm ; SiC: ~ 3 MV/cm).



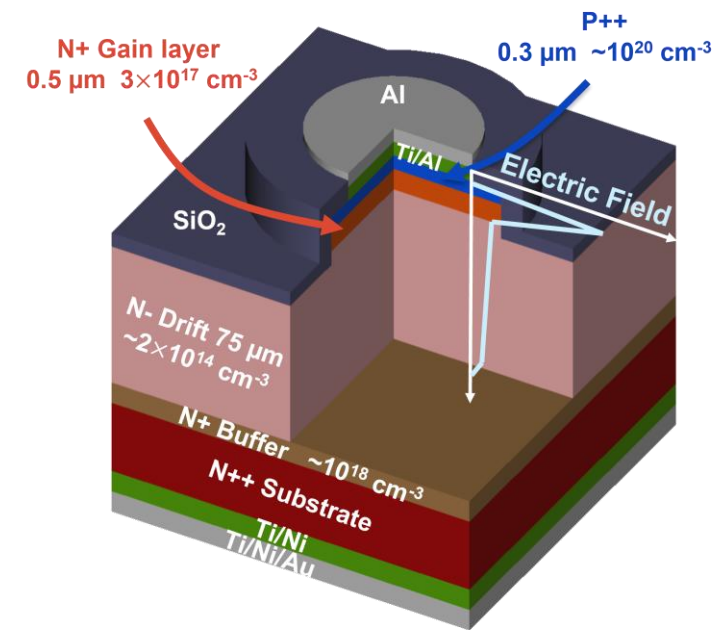
I-V & C-V Comparison of PIN and LGAD

- The wafer (W2) with 4H-SiC epitaxial stacks having specific doping concentrations, which exhibit the typical electric field distribution of LGADs.
- For comparison, the wafer (W5) is without gain layer, resulting in a typical PIN electric field distribution.
- The measurements:
 - Both LGAD and PIN have high breakdown voltages.
 - Lower breakdown voltage and higher leakage current of LGAD are observed comparing PIN

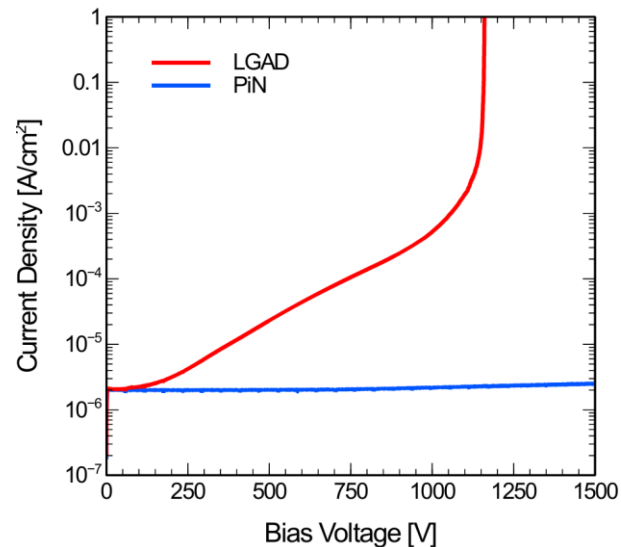
4H-SiC PIN (W5)



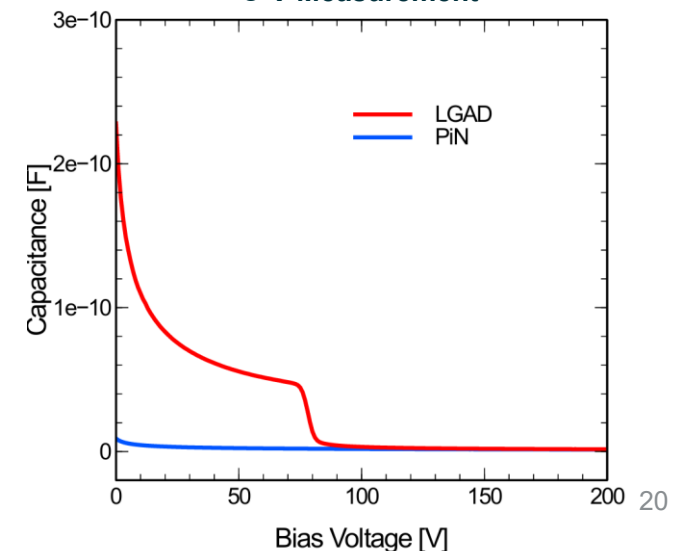
4H-SiC LGAD (W2)



I-V Measurement



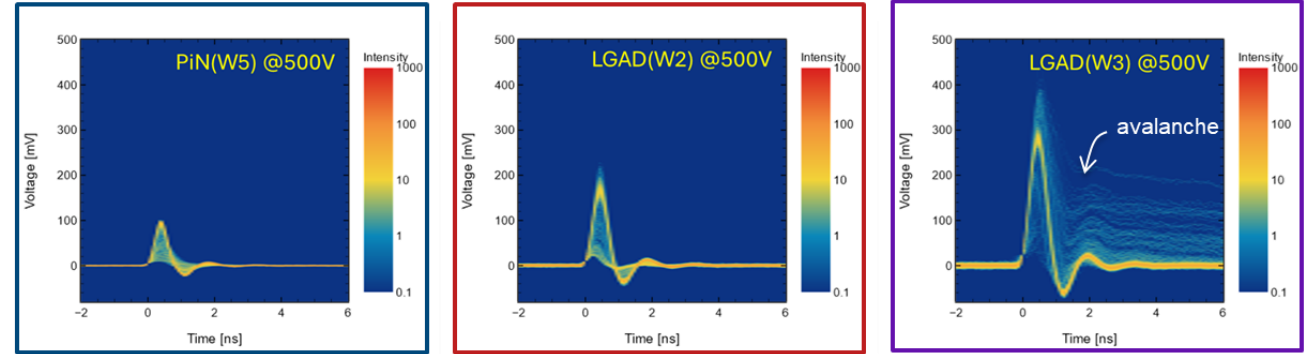
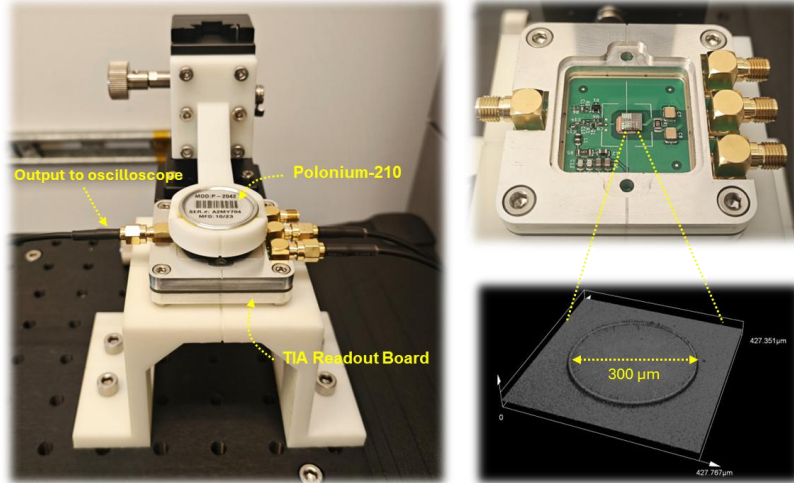
C-V Measurement



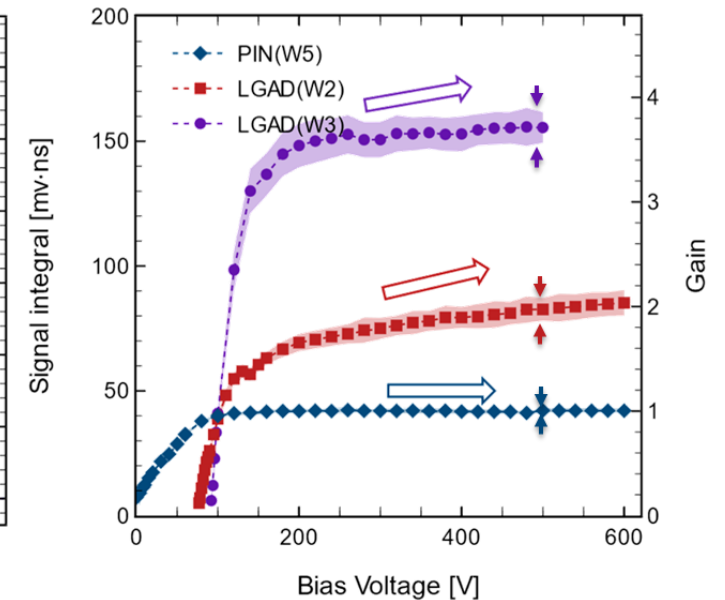
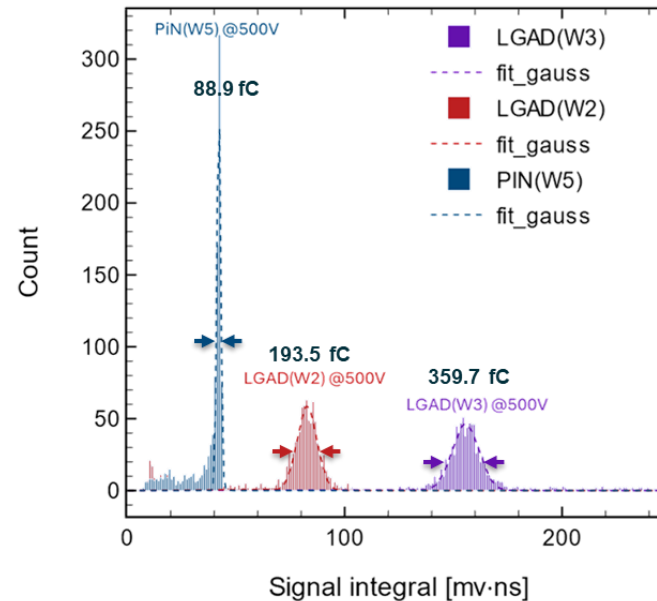
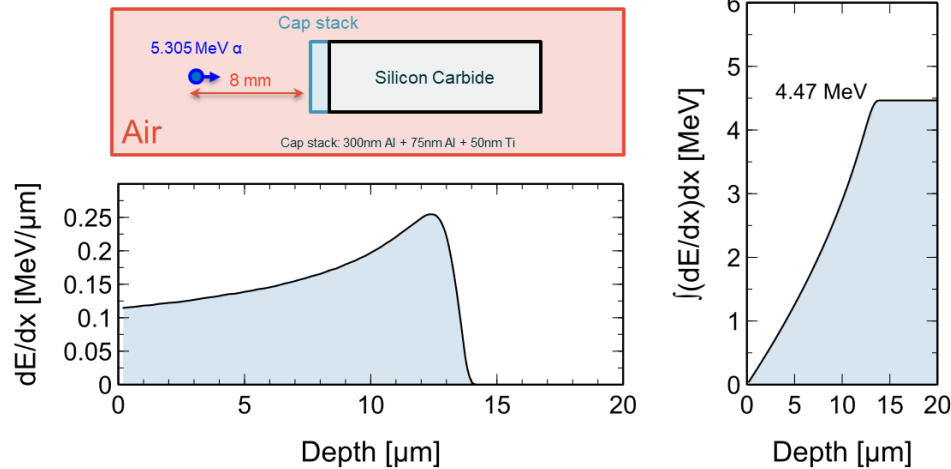
Response of α particles from ^{210}Po Source

✓ Evidence of the low gain carrier multiplication

Test Setup

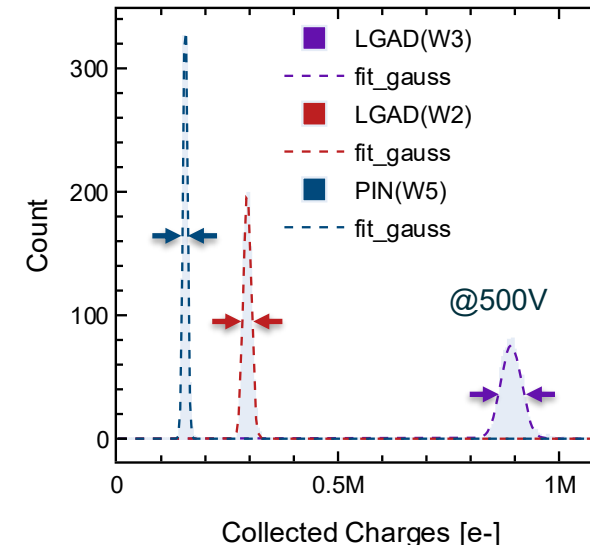
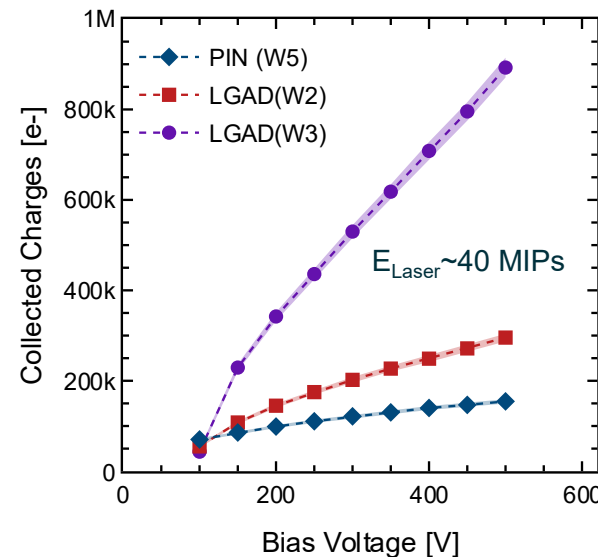
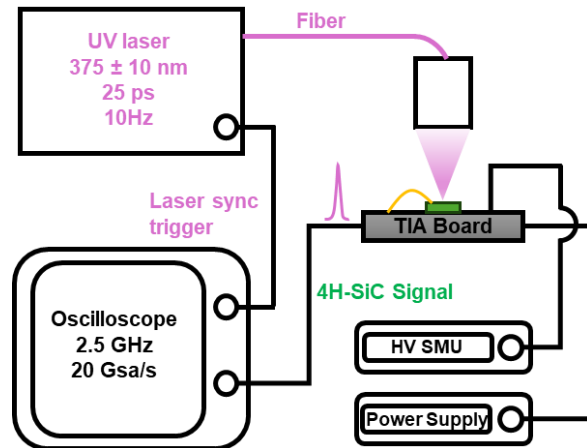
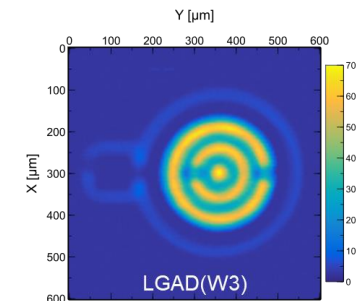
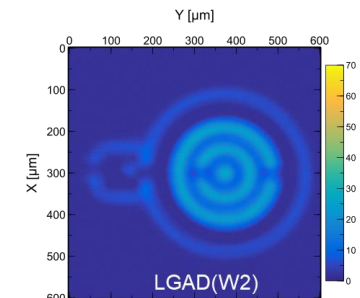
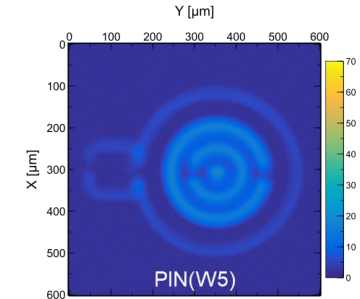
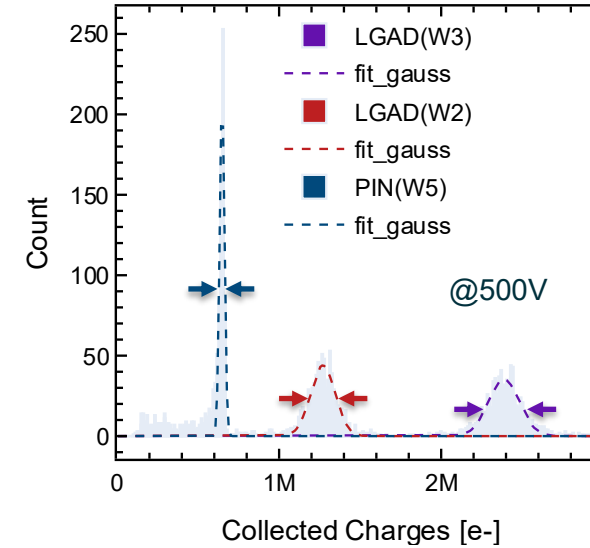
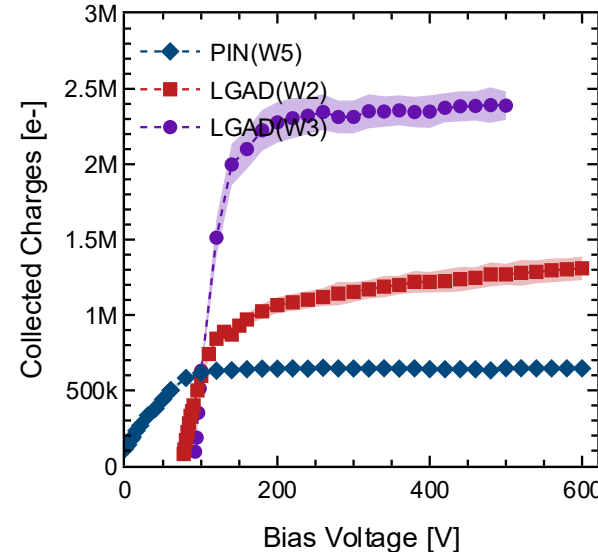
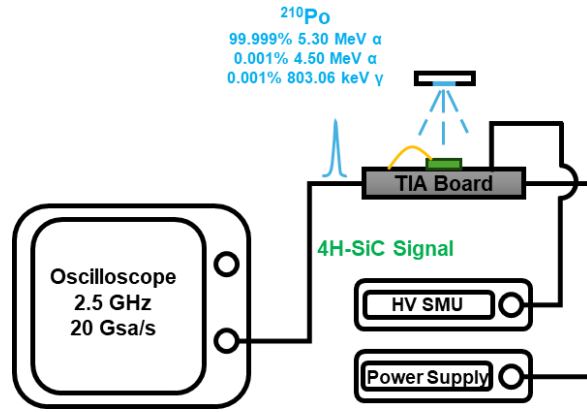


SRIM Simulation

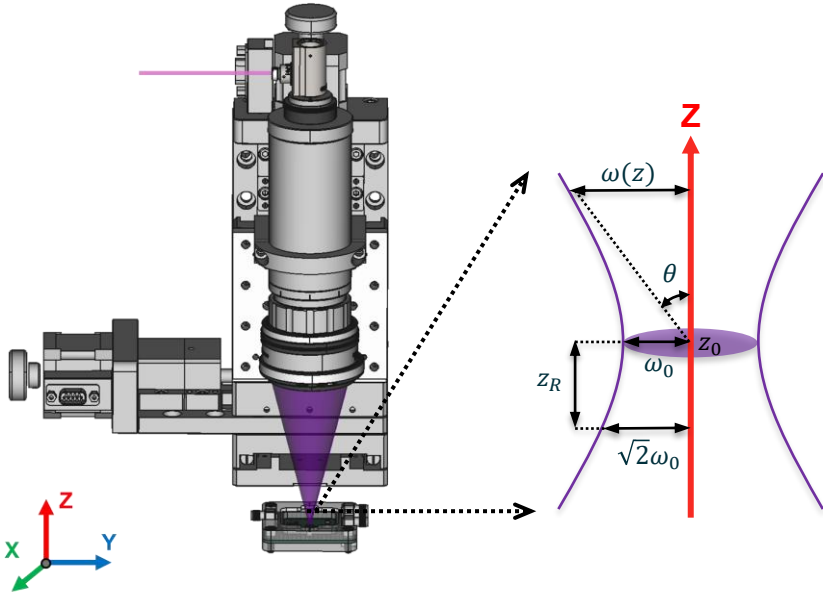


Charges Collection for Different Gain layer Doping Concentration

- As expected, a higher doping concentration of the gain layer has a larger gain.
- Higher gain exhibits **greater multiplication randomness**, resulting in a **wider charge collection distribution**.



Characterization of the Laser Beam Profile



Based on the TEM₀₀ Gaussian mode, the intensity distribution of a Gaussian beam:

$$I(r, z) = I_0 \frac{\omega_0^2}{\omega^2(z)} \exp\left(-\frac{2r^2}{\omega^2(z)}\right) \quad \omega(z) = \omega_0 \sqrt{1 + \left(\frac{z - z_0}{z_R}\right)^2}$$

where r is the radial coordinate and I_0 defines the intensity in the center of the beam focus. $\omega(z)$ describes the dependency of the width of the laser beam on the z -position. The spot size has a minimum at $z = z_0$, z_R is the Rayleigh length.

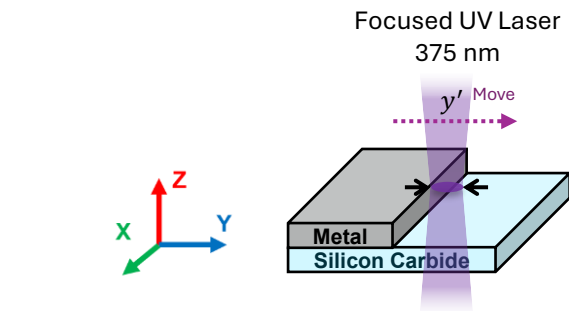
For the laser beam is moved into the knife edge on the y -direction, if the knife edge at $y = 0$, the measured intensity I_m when the laser beam at y' is

$$I_m(y', z) = \int_{y'}^{+\infty} dy \int_{-\infty}^{+\infty} I(x, y, z) dx = I_0 \frac{\omega_0^2}{\omega^2(z)} \int_{y'}^{+\infty} dy \int_{-\infty}^{+\infty} \exp\left(-\frac{2(x^2 + y^2)}{\omega^2(z)}\right) dx$$



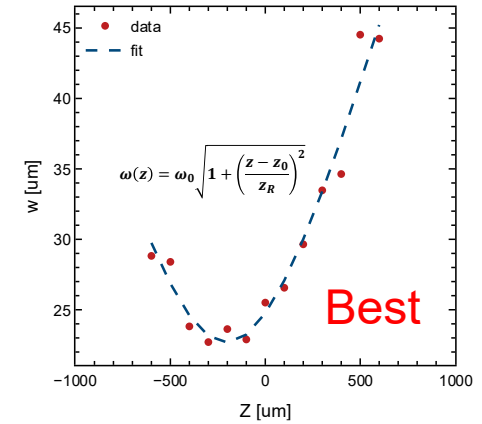
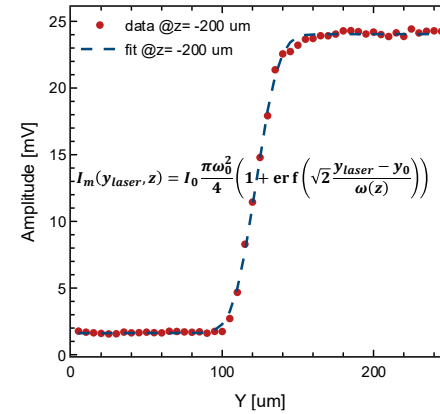
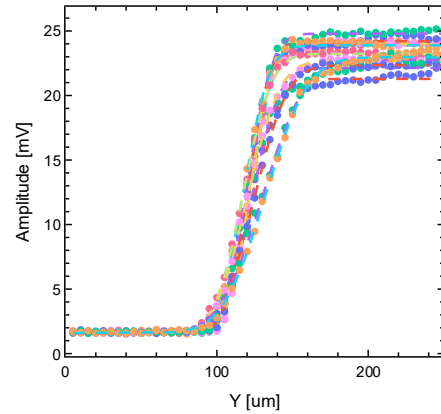
$$I_m(y_{laser}, z) = I_0 \frac{\pi \omega_0^2}{4} \left(1 + \operatorname{erf}\left(\sqrt{2} \frac{y_{laser} - y_0}{\omega(z)}\right)\right)$$

where y_{laser} is the position of laser beam and y_0 is the position of the knife edge.

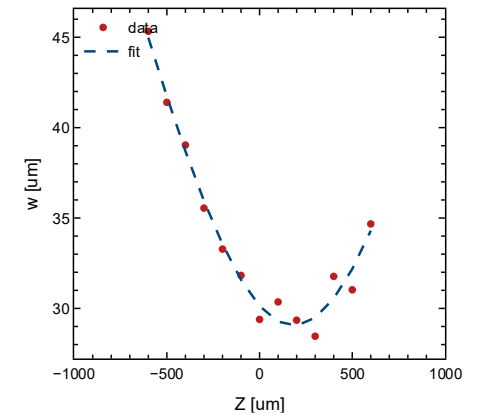
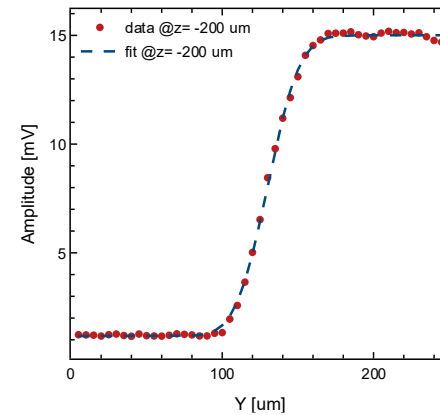
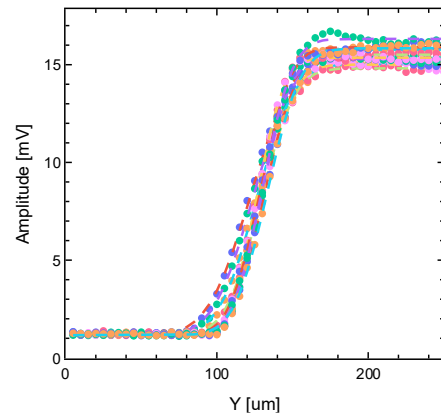


Laser Beam Profile by different lens

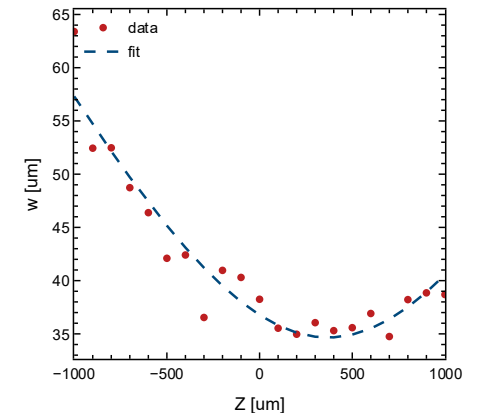
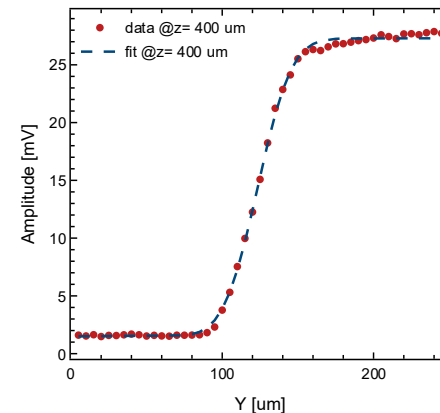
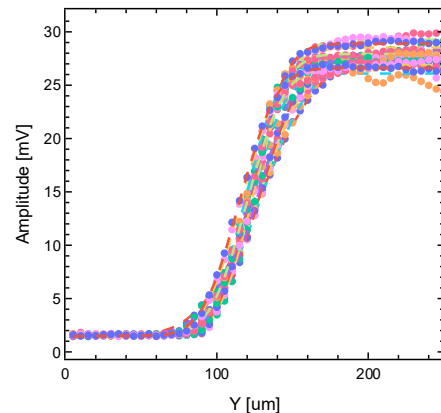
Plano-Convex
 Ø2", f = 60 mm



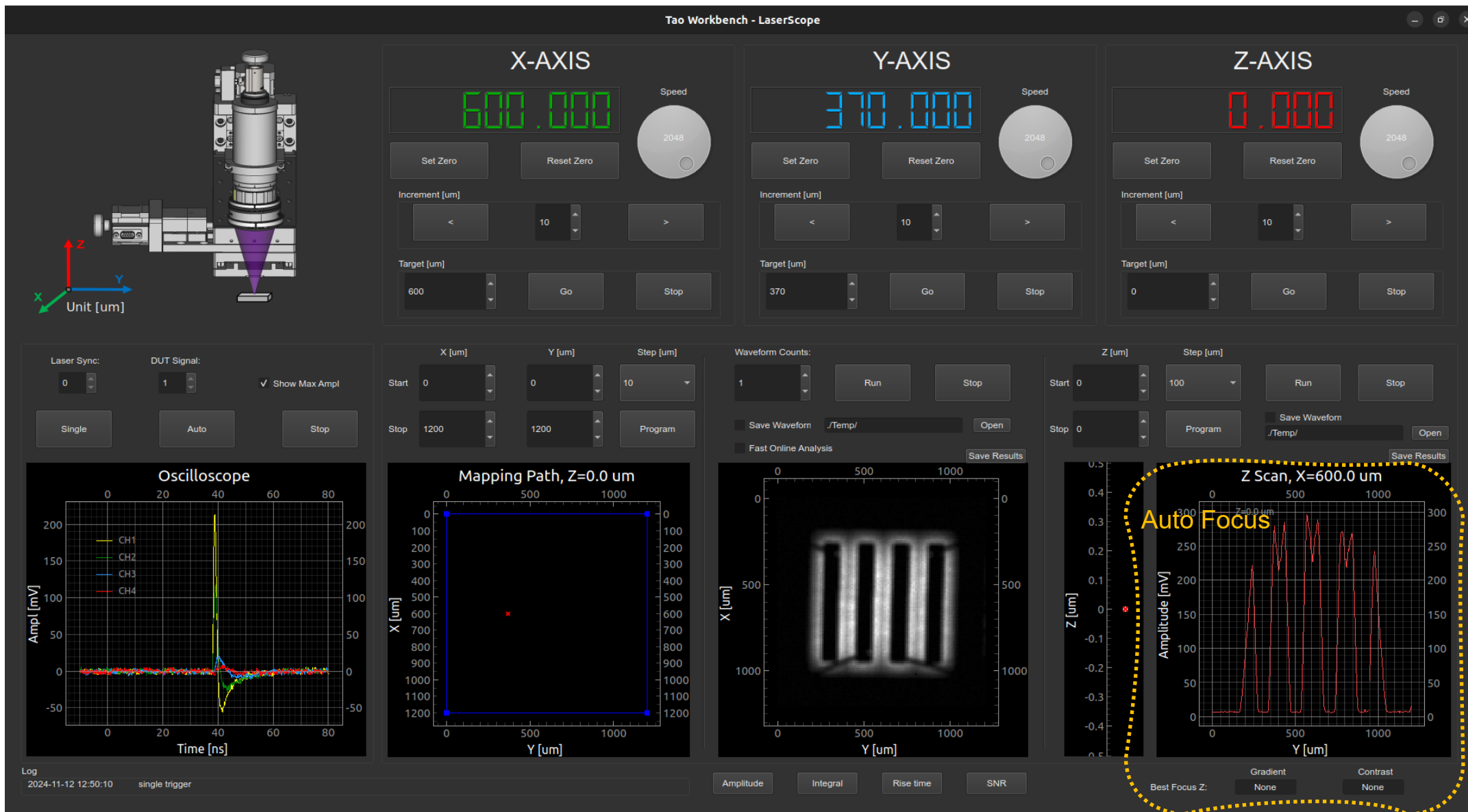
Achromatic Doublets
 Ø2", f = 75 mm



Plano-Convex
 Ø2", f = 100 mm

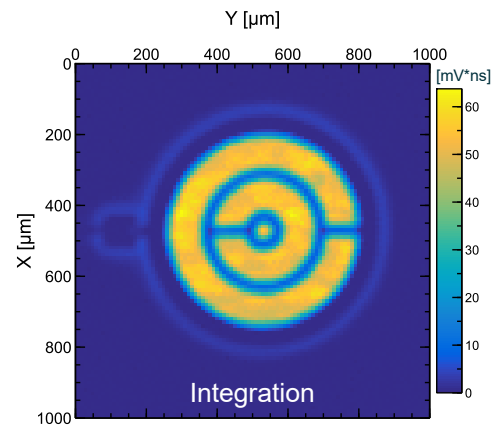
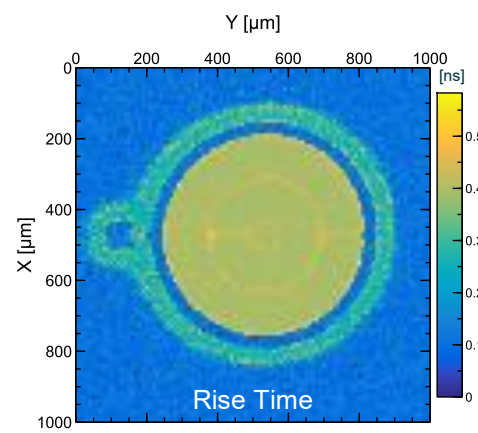
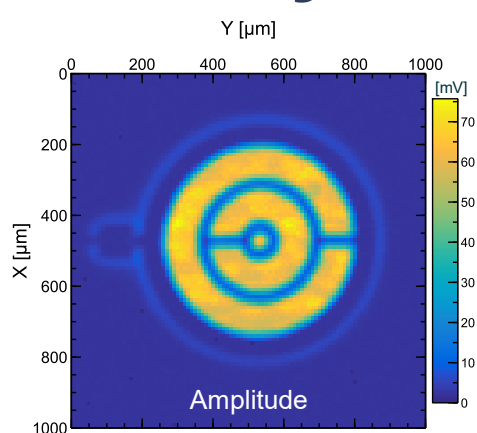
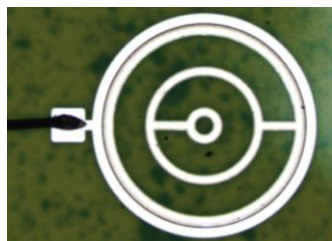


LaserScope GUI for UV-TCT

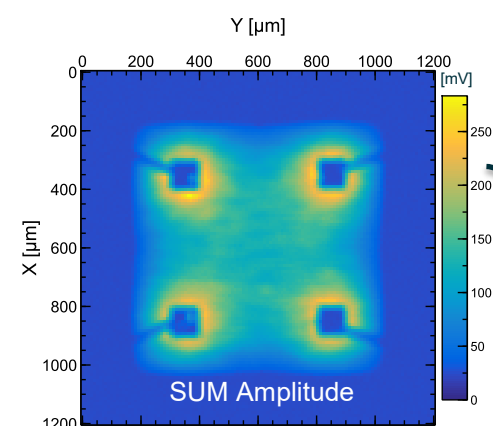
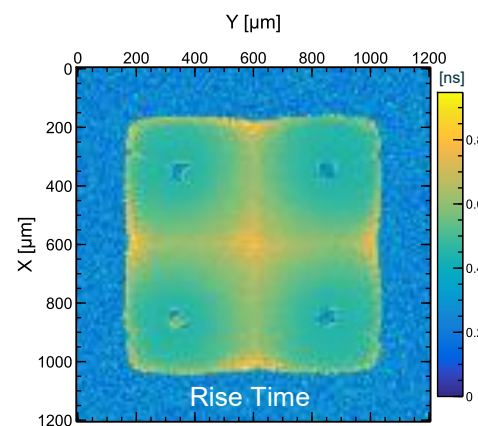
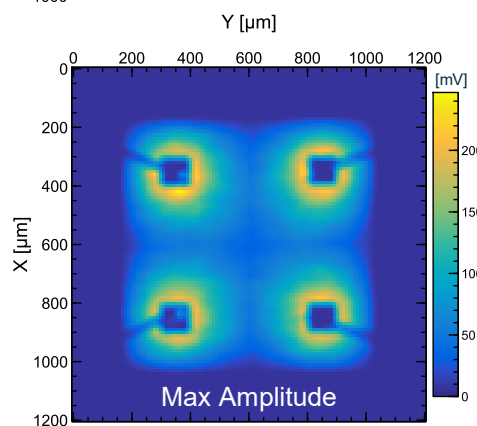
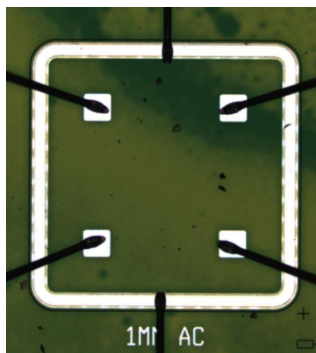


Scanning Results by UV-TCT

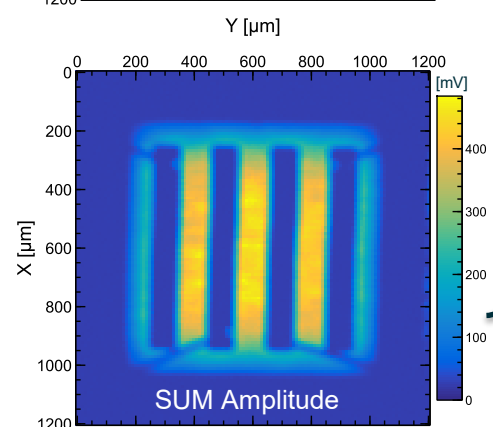
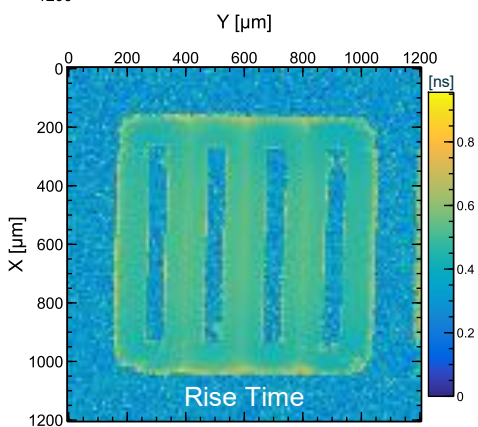
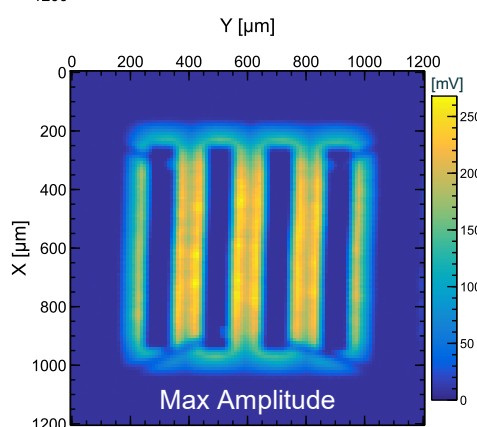
600 μm SiC DC-LGAD



1mm SiC Pixel AC-LGAD



1mm SiC Strip AC-LGAD

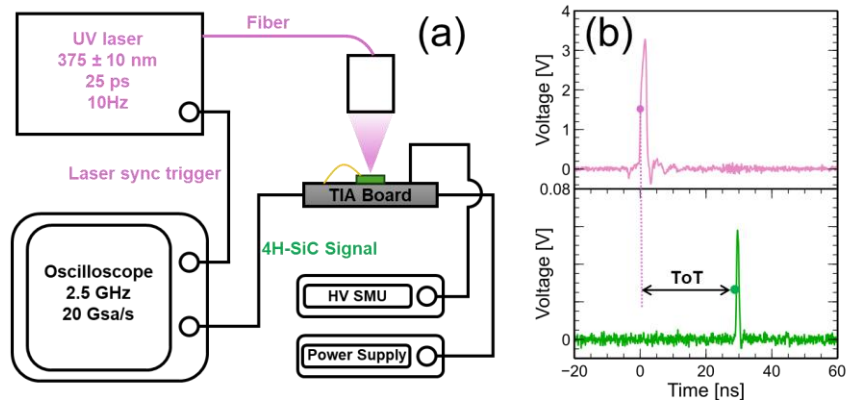


- **Amplitude:** the maximum peak value of signal pulse.
- **Rise Time:** the time interval from 10% to 90% of amplitude.
- **Integration:** the time integral of the pulse signal from TIA.

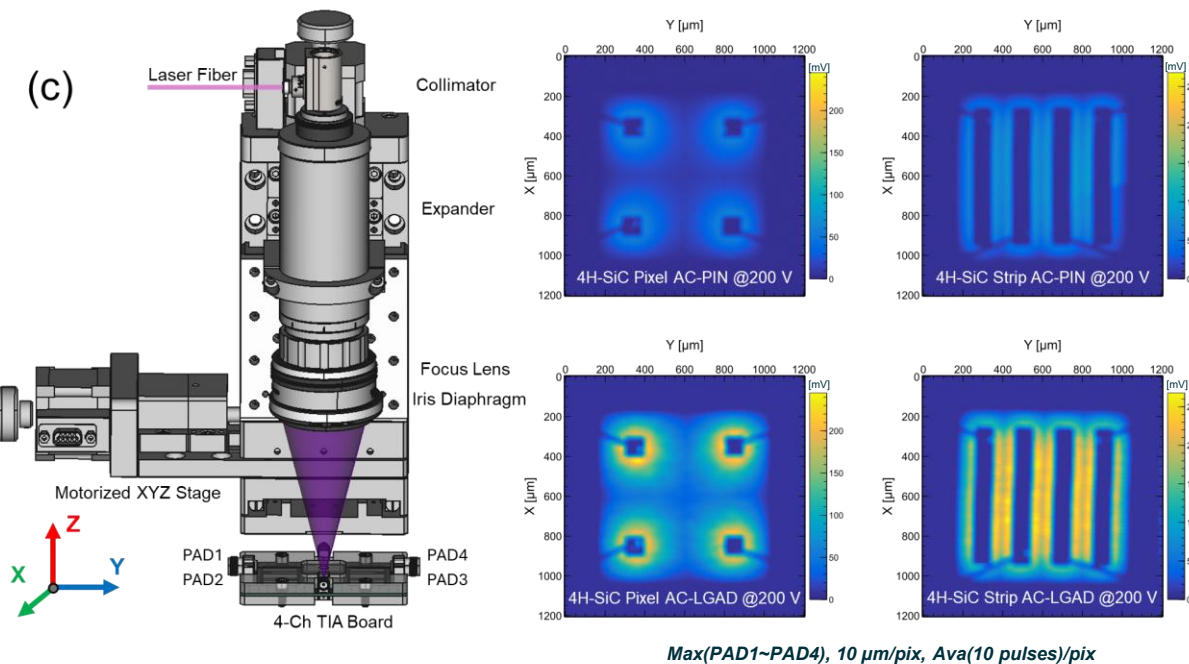
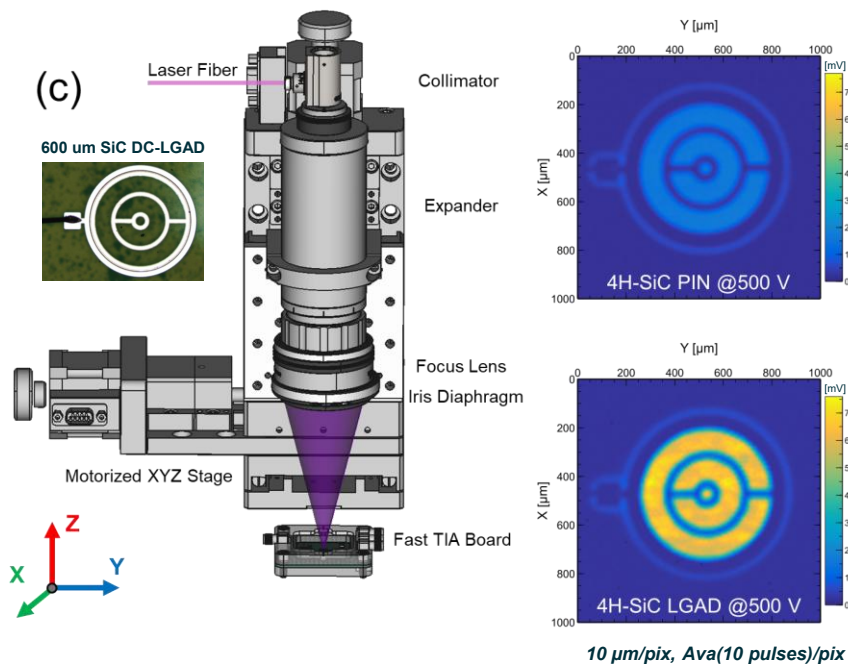
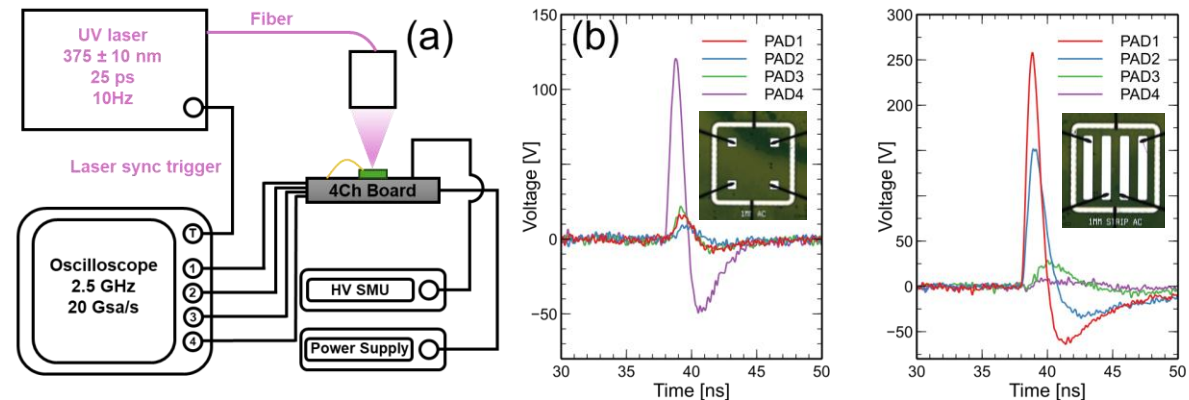
- **Max Amplitude:** the maximum amplitude in four AC-PADs.
- **Rise Time:** the rise time of the signal pulse that the PAD has the maximum amplitude.
- **SUM Amplitude:** the sum of the amplitudes from the four AC-PADs.

Ultraviolet Transient Current Technique (UV-TCT)

Single Channel for SiC DC-LGAD / PIN



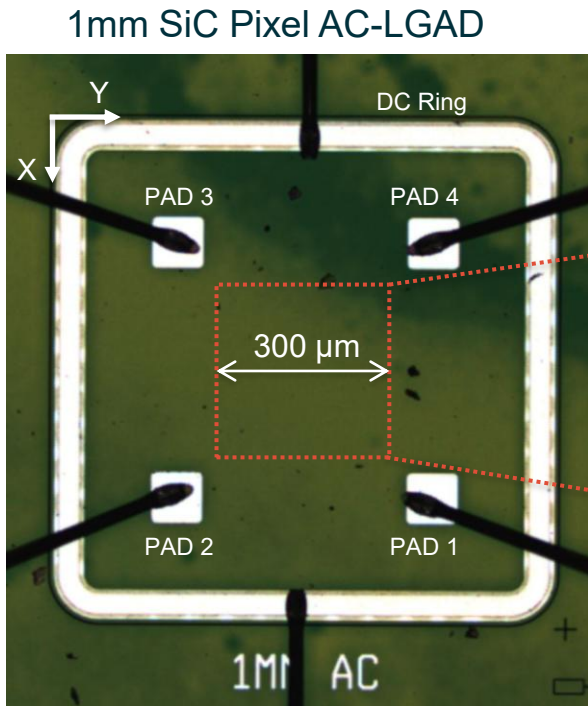
Four Channels for SiC AC-LGAD / PIN



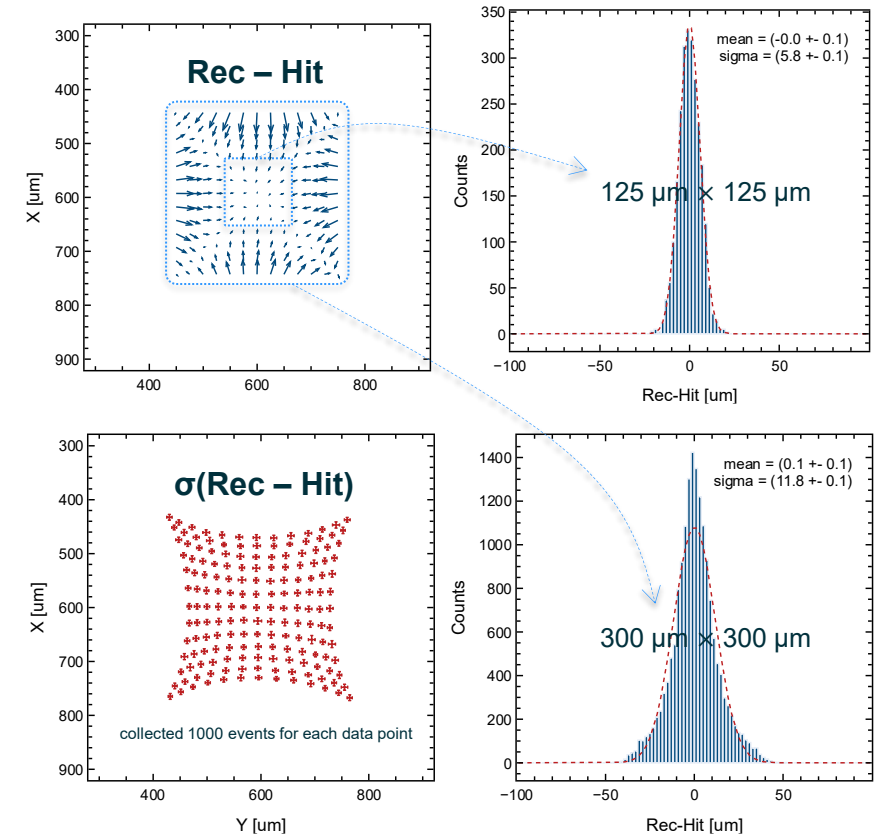
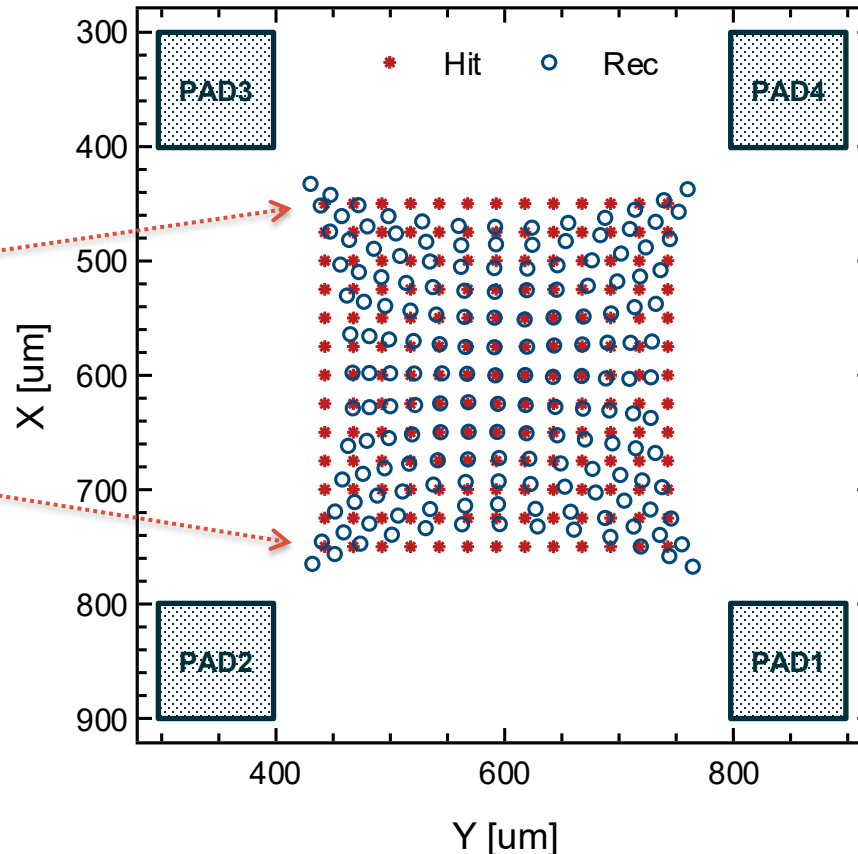
Position Resolution of SiC AC-LGAD

- The SiC AC-LGAD demonstrates good position resolution with $\sigma = 5.8 \mu\text{m}$ in the central region.
- The reconstructed position near the edges currently exhibits distortion due to limitations in the reconstruction algorithm (pad shape and charges leakage by DC-Ring), this issue can be addressed through **algorithm optimization** and **electrode shape optimization**.

$$\sigma_P^2 = \sigma_A^2 + \sigma_{jitter}^2 + \sigma_{algorithm}^2 + \sigma_{sensor}^2 + \cancel{\sigma_{MIPs}^2}$$

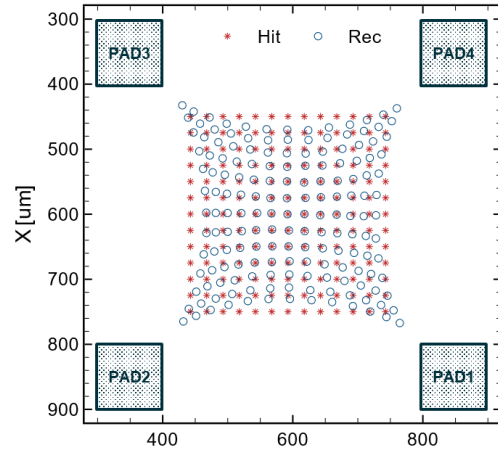
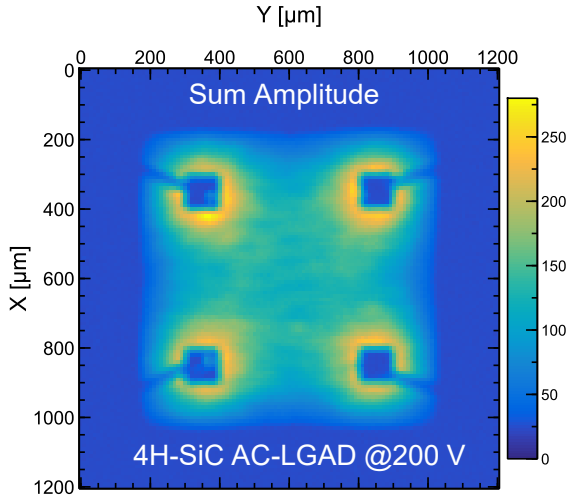


Reconstructed position by Discretized Positioning Circuit (DPC) Method



The Influence of Geometric Factors

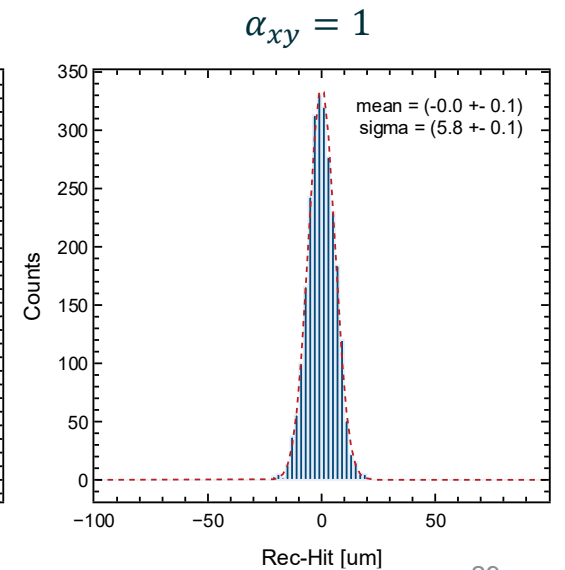
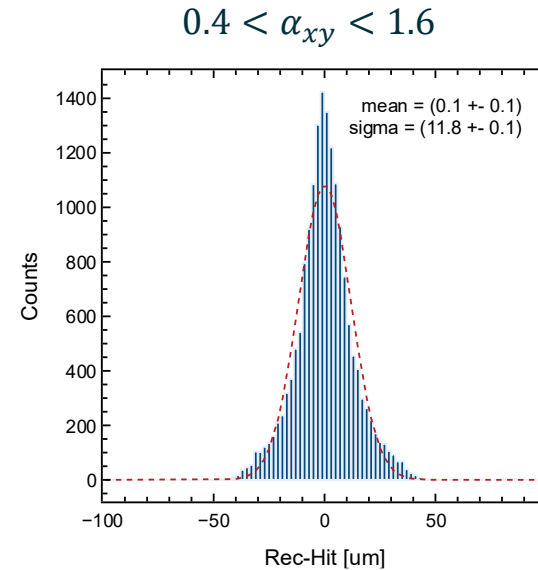
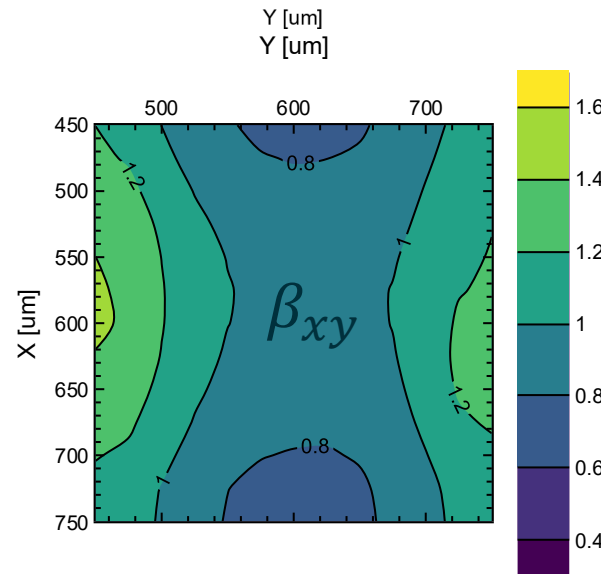
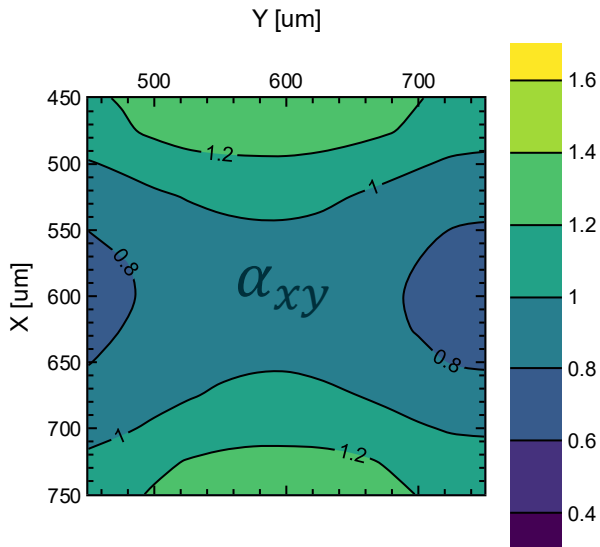
Due to charge leakage into the DC ring in the edge region, the reconstructed position is distorted.



$$\begin{cases} x_{\text{Rec}} = x_0 + k_x m \\ m = \frac{a_1 + a_2 - a_3 - a_4}{a_1 + a_2 + a_3 + a_4} \\ k_x = l \frac{\sum (m_{i+1} - m_i)}{\sum (m_{i+1} - m_i)^2} \alpha_{xy} \end{cases} \quad \begin{cases} y_{\text{Rec}} = y_0 + k_y n \\ n = \frac{a_1 + a_4 - a_2 - a_3}{a_1 + a_2 + a_3 + a_4} \\ k_y = l \frac{\sum (n_{i+1} - n_i)}{\sum (n_{i+1} - n_i)^2} \beta_{xy} \end{cases}$$

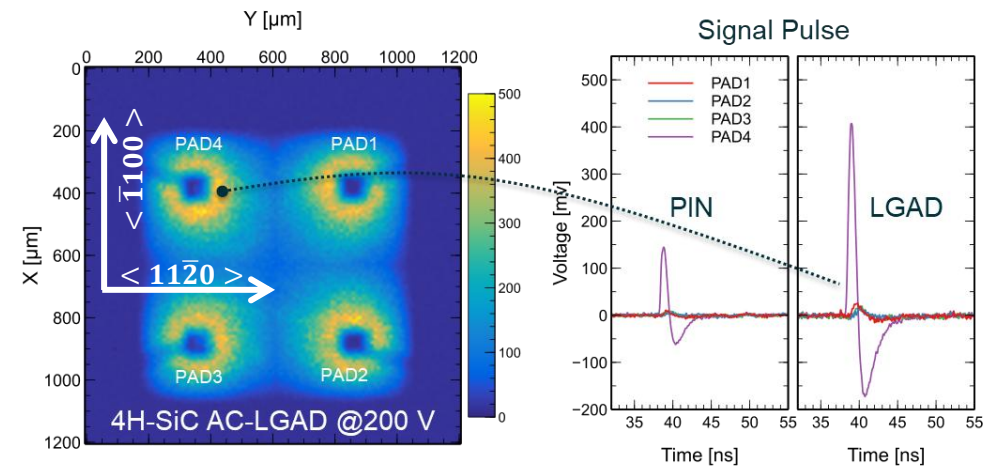
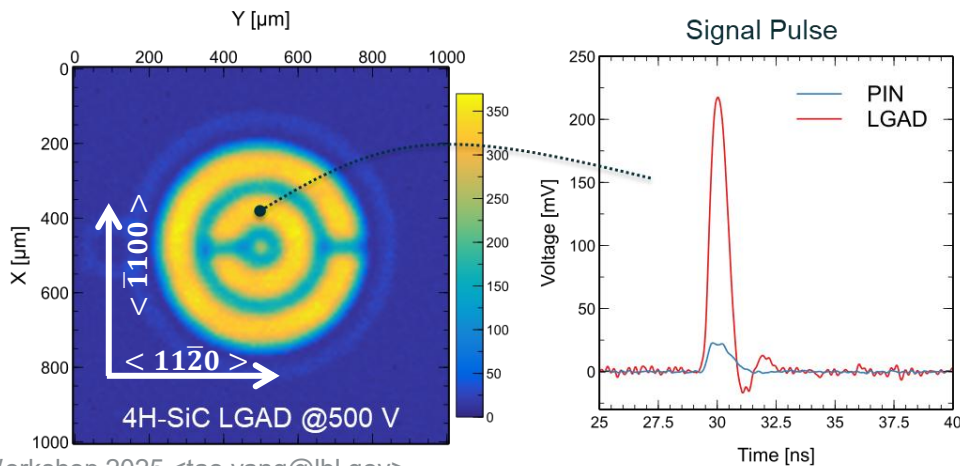
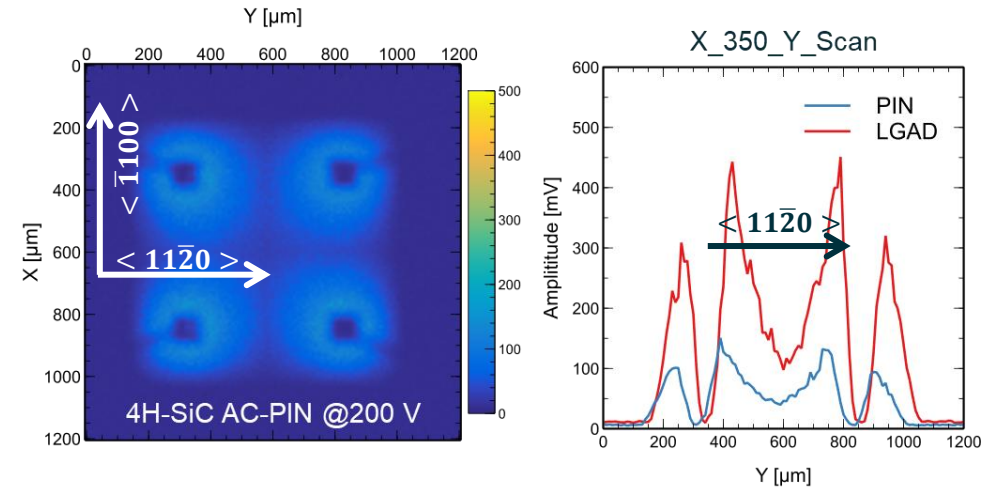
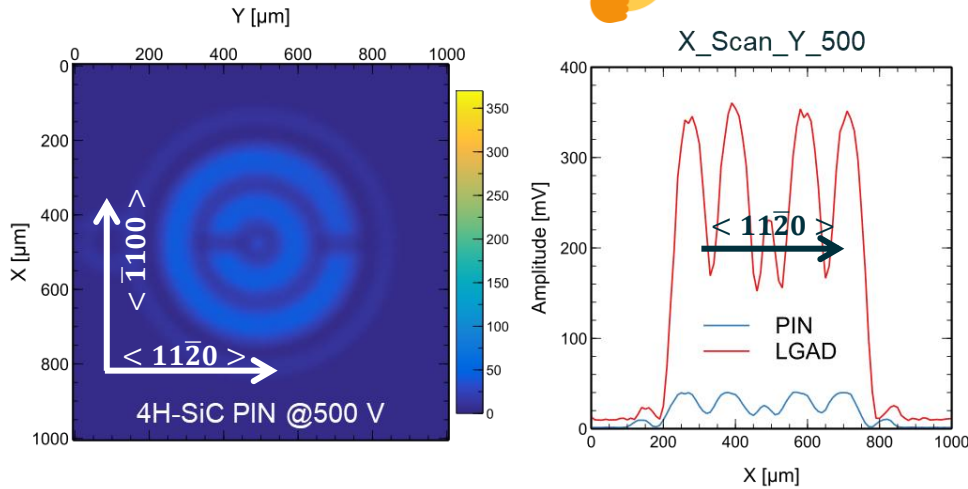
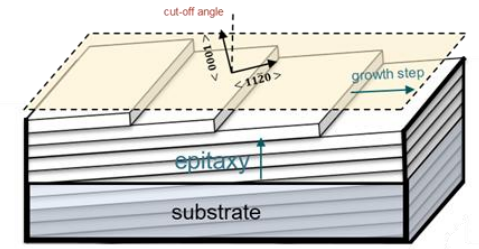
Where a_1, a_2, a_3, a_4 represent the signal amplitudes induced on the four ac pads.

α_{xy} and β_{xy} are **geometric factor**. The region with geometric factor ~ 1 exhibits the best position resolution.



Gain Uniformity

- Unlike the avalanche anisotropy along the $\langle 11\bar{2}0 \rangle$ direction reported in some studies of SiC APDs due to the cut-off angle, no significant anisotropy has been observed in SiC LGADs
- This suggests that anisotropy may only become apparent in avalanche processes at very high gain, requiring further investigation. 🤔 ?



Gain Spatial Nonuniformity of 4H-SiC APD

* Note : Gain measured by current

[Sampath, Anand V., et al. 2023.](#)

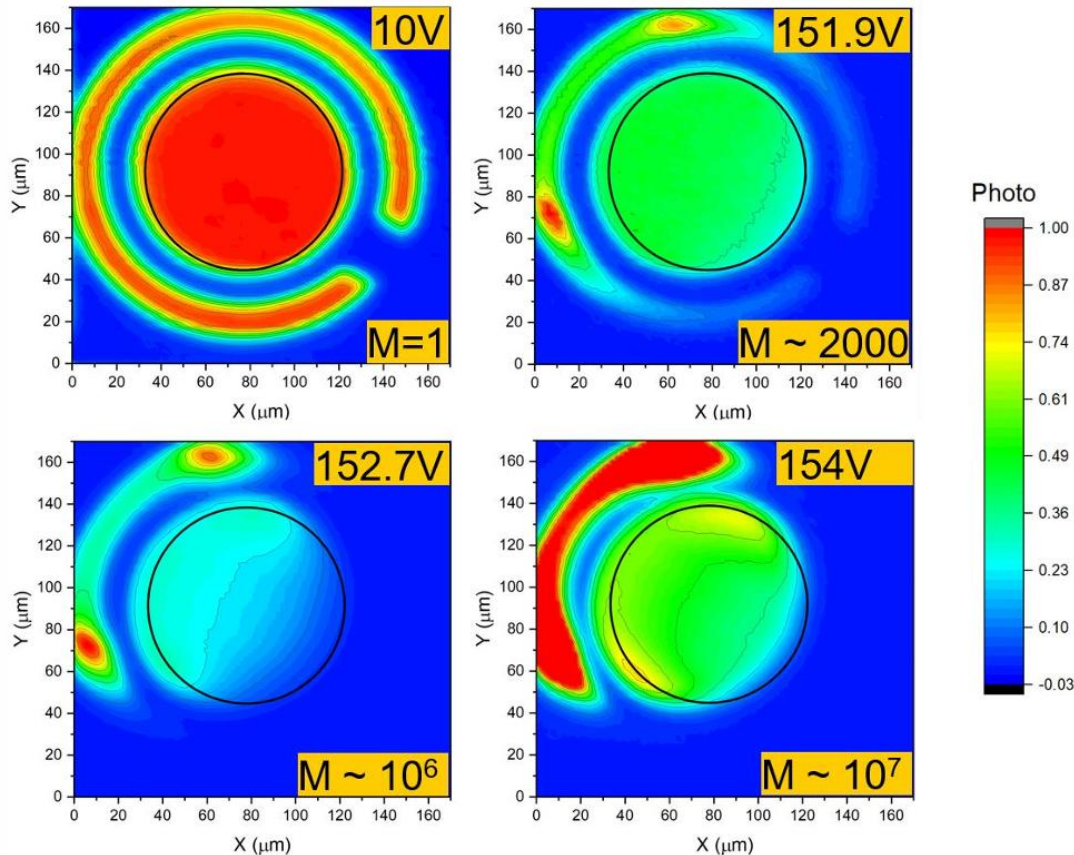


Figure 2. Optical microscope image (top) and linear-mode spatial response measurement of p-i-n SiC APD (bottom) at various levels of multiplier gain (M). Black circle identifies the photosensitive area of the APD at unity-gain.

[Li, Tianyi, et al. 2024.](#)

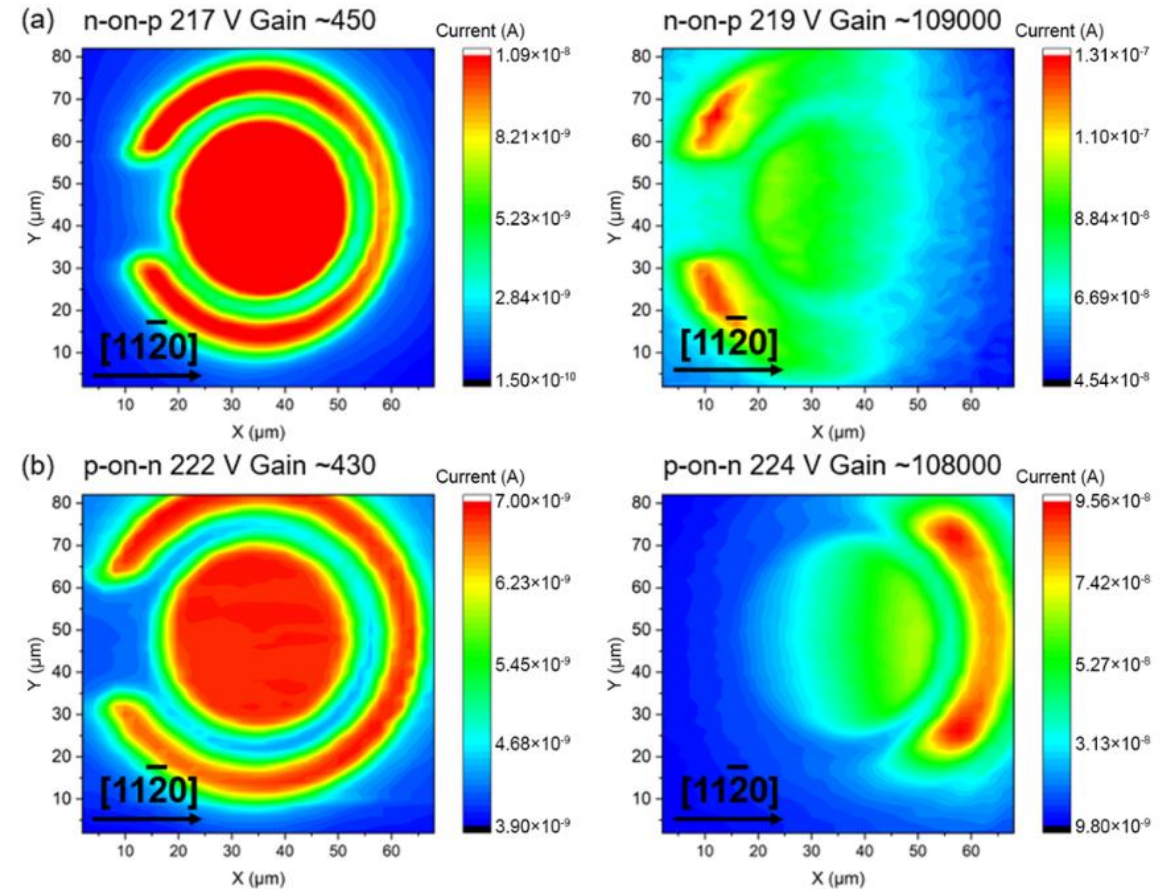
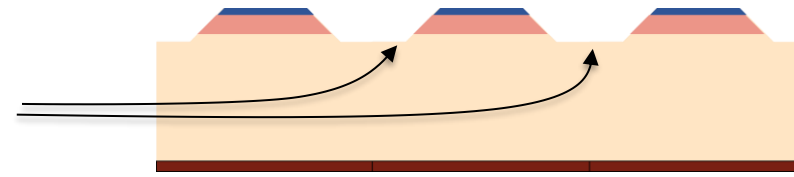
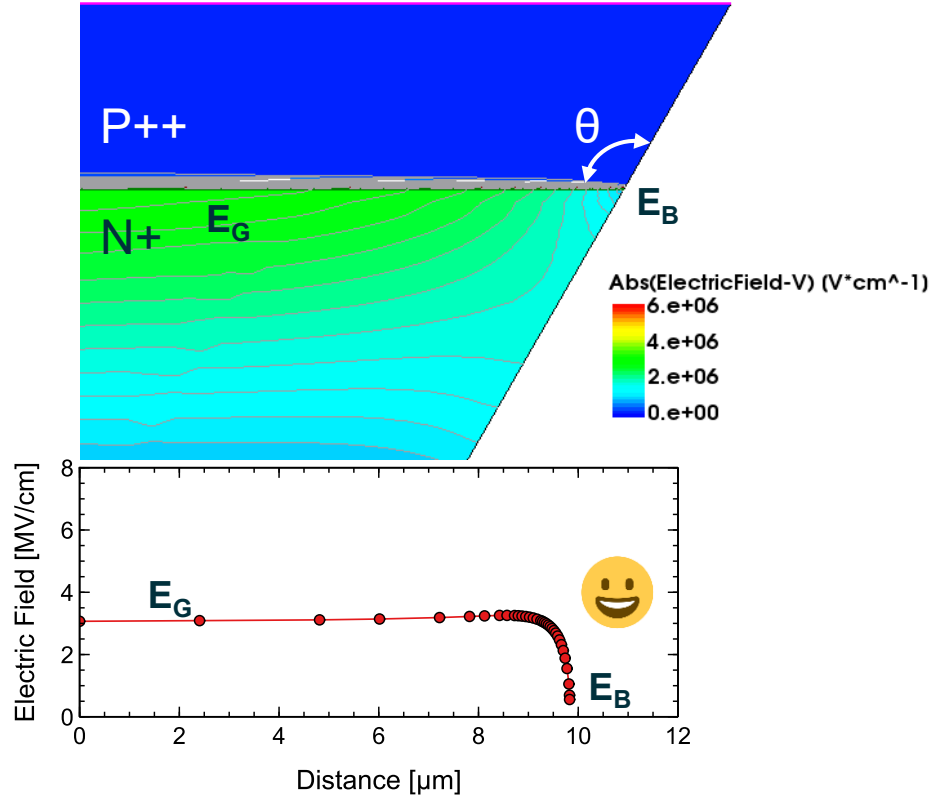


Fig. 2. Two-dimensional photocurrent mapping of the (a) n-on-p and (b) p-on-n APDs at different gains.

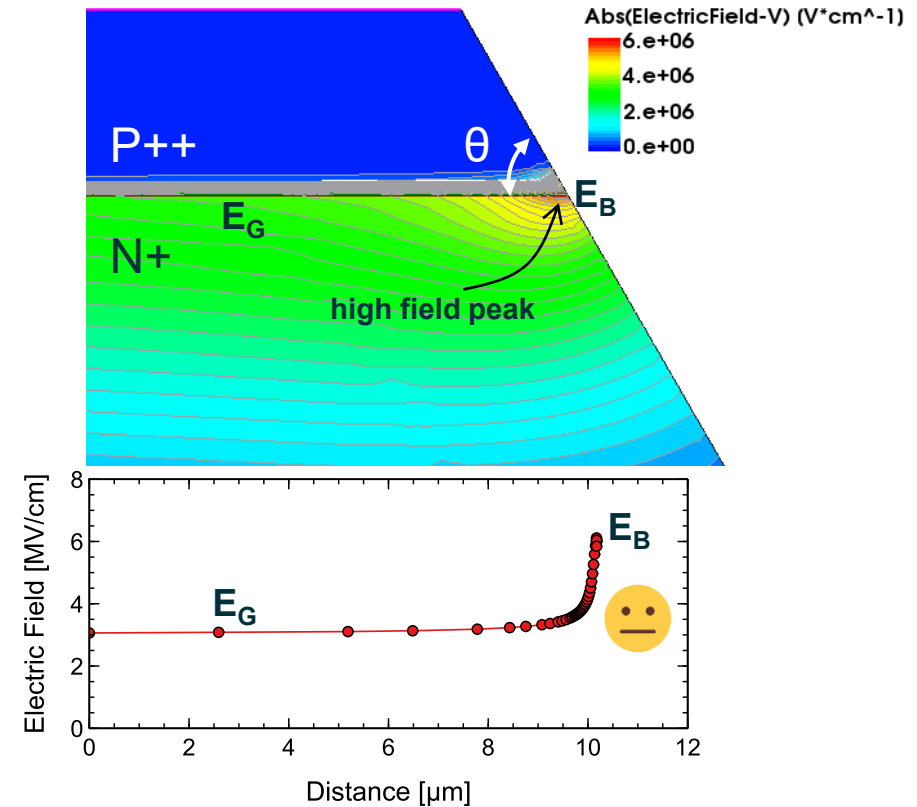
Bevel Termination

Etched bevel termination for device isolation

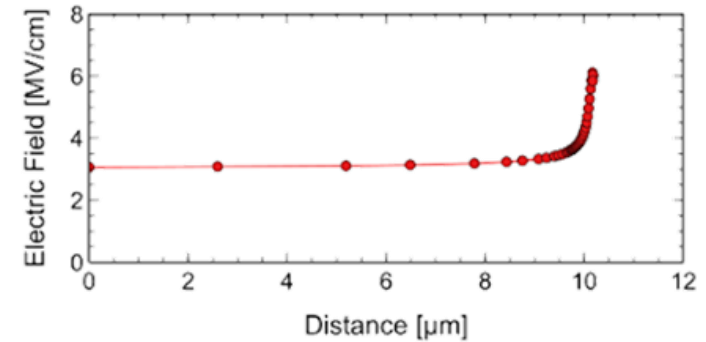
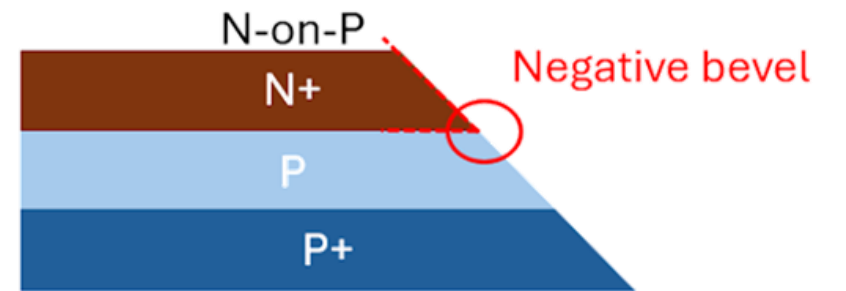
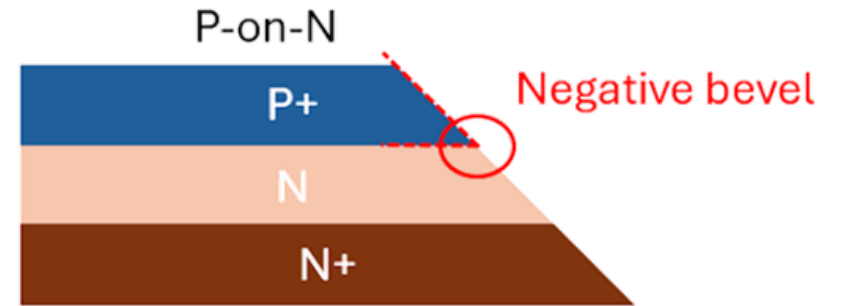
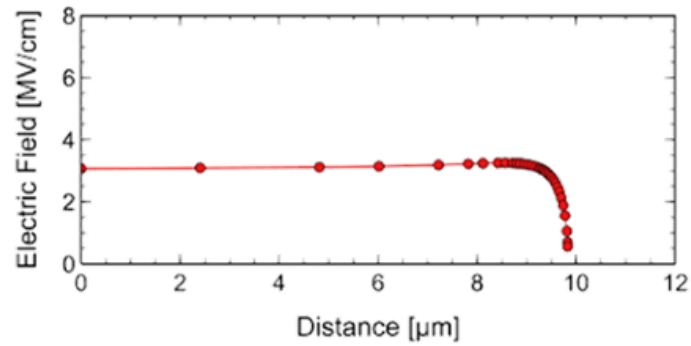
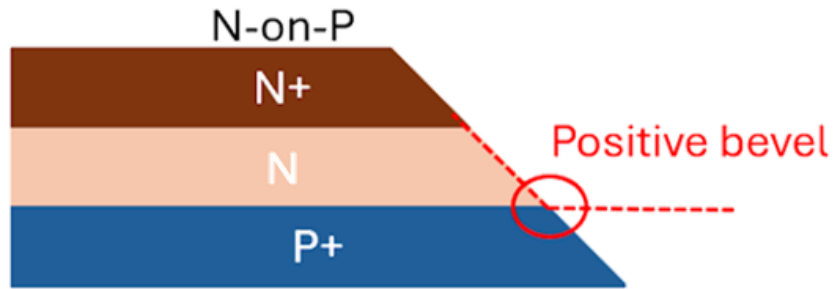
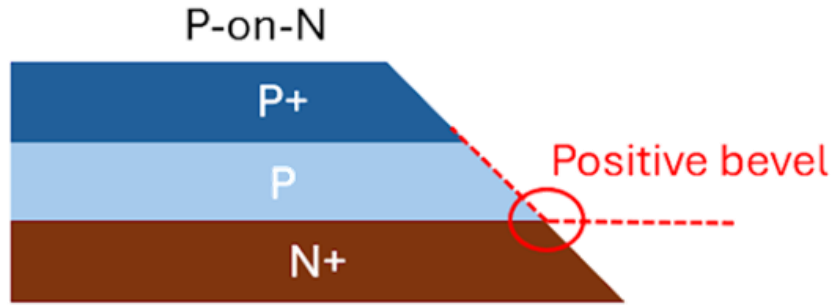
- **Positive bevel ($\theta > 90^\circ$) :**
more material is removed from the highly doped side to the lightly doped side of the PN junction.



- **Negative bevel ($\theta < 90^\circ$) :**
less material is removed from the highly doped side to the lightly doped side of the PN junction.

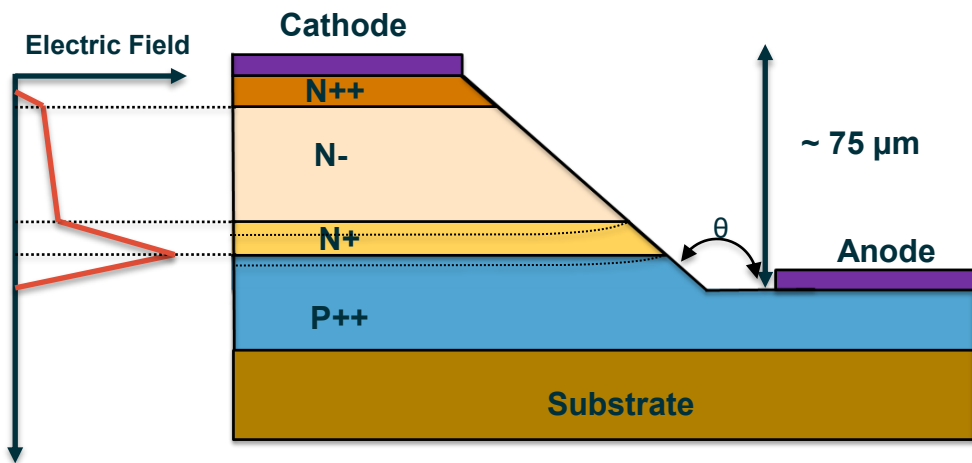


Bevel Termination



SiC LGAD with Bevel Termination

- Ideal SiC LGAD with positive bevel termination



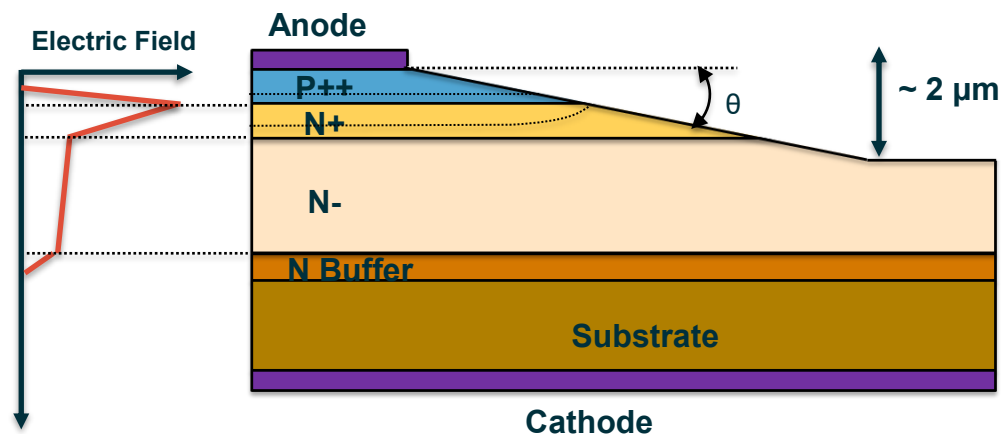
Feature:

Positive bevel termination with maximizing the breakdown voltage.

Difficulty:

Difficult to achieve $\sim 75 \mu\text{m}$ bevel etch with existing technology.

- Realizable SiC LGAD with negative bevel termination



Feature:

Could achieve $\sim 2 \mu\text{m}$ bevel etching with existing technology.

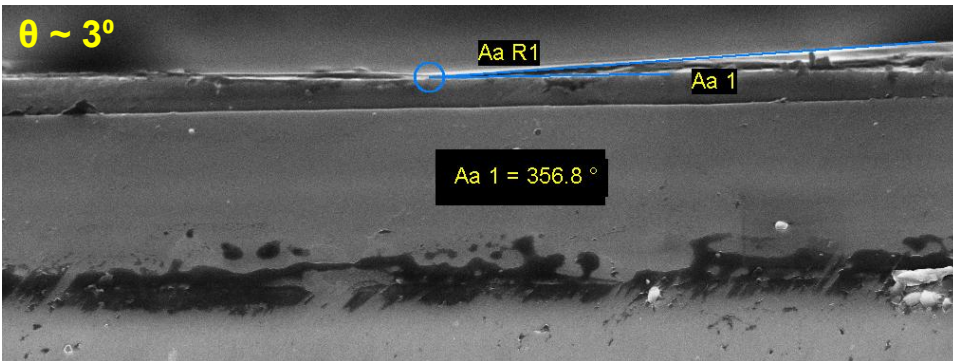
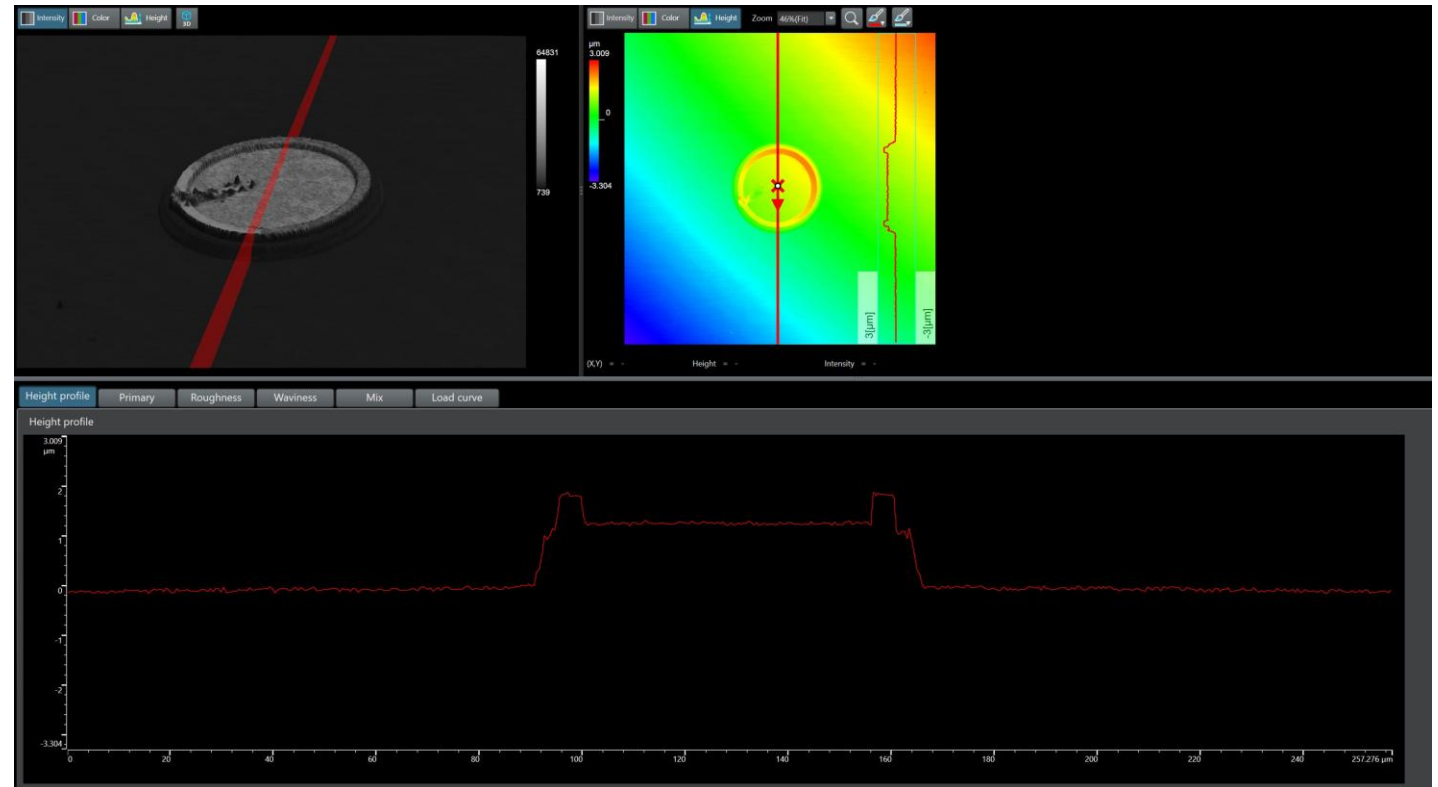
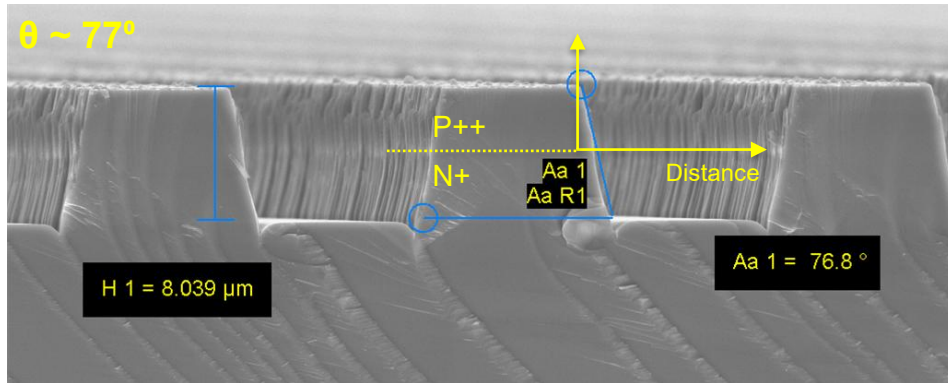
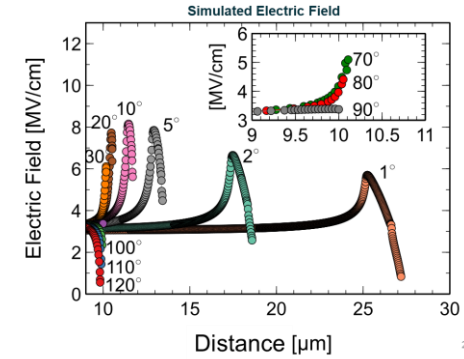
Difficulty:

The electric field at the bevel surface will be larger than the field in the bulk. It is easy to cause early breakdown of the device.

Etched Termination Measurement

- To maximize the breakdown voltage, two methods can be used based on the existing silicon carbide process technology:

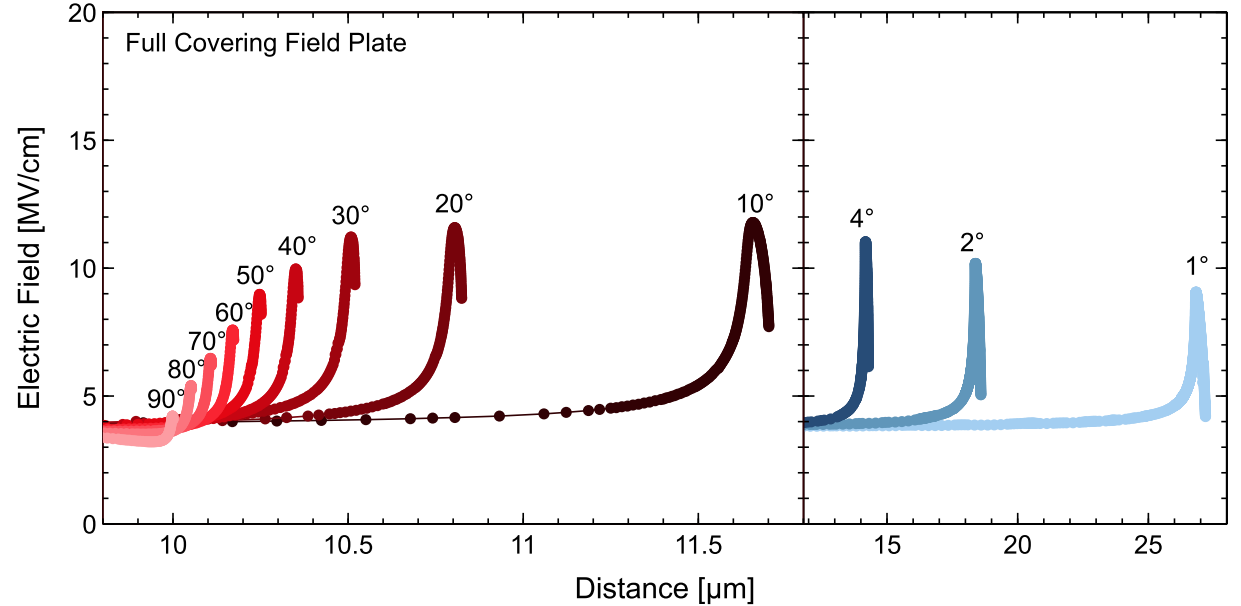
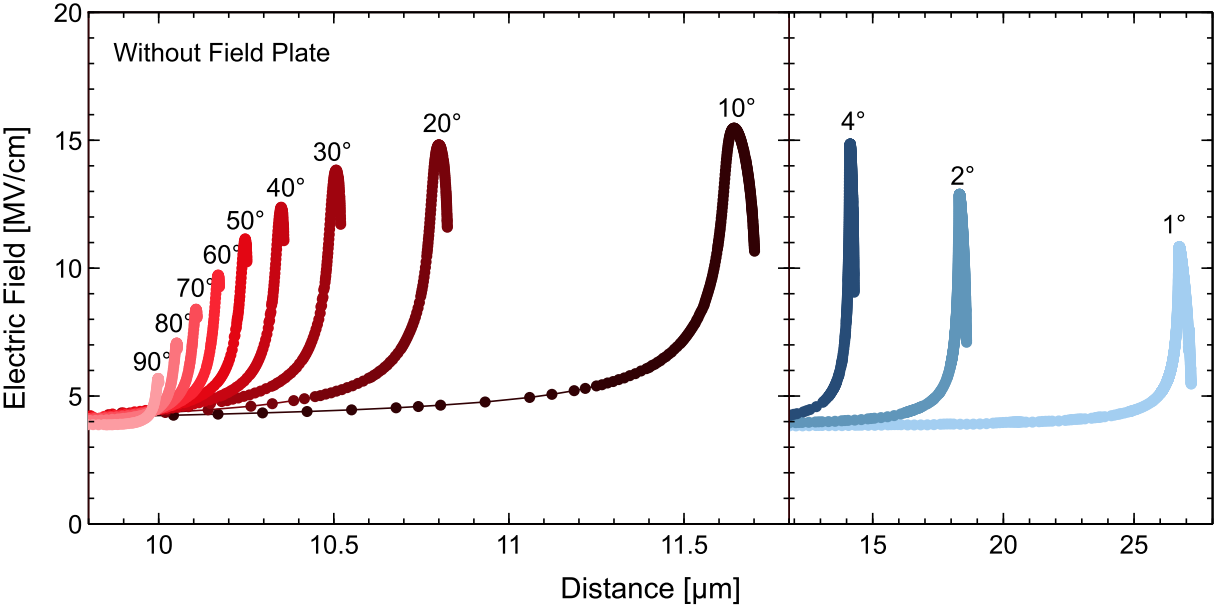
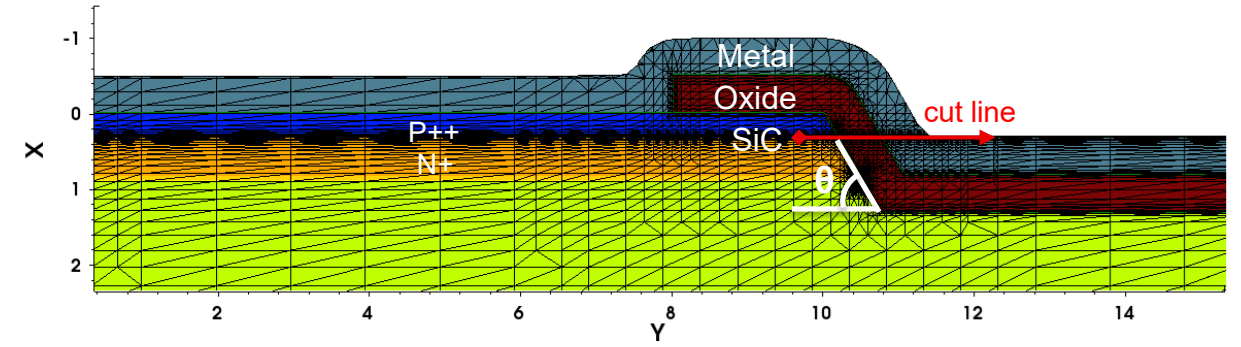
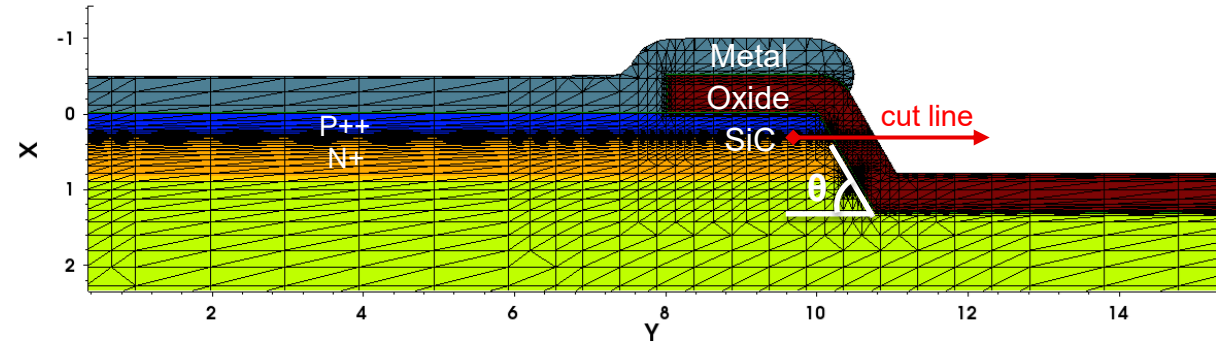
- 1) make the angle as close to 90° as possible.
- 2) make the angle as small as possible, less than 5° .



lower electric field at bevel with vertical etching ($\theta = 90^\circ$) or extremely small angle ($\theta < 2^\circ$).

- The equipotential lines are reformed to parallel with the surface by the extended field plate.

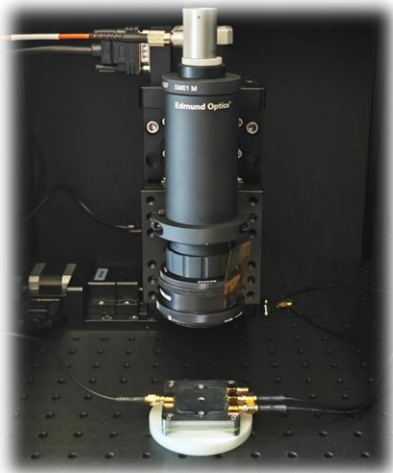
* Note: limited by grid meshing accuracy for extremely small angle, the simulated results for $1^\circ \sim 2^\circ$ are for reference only.



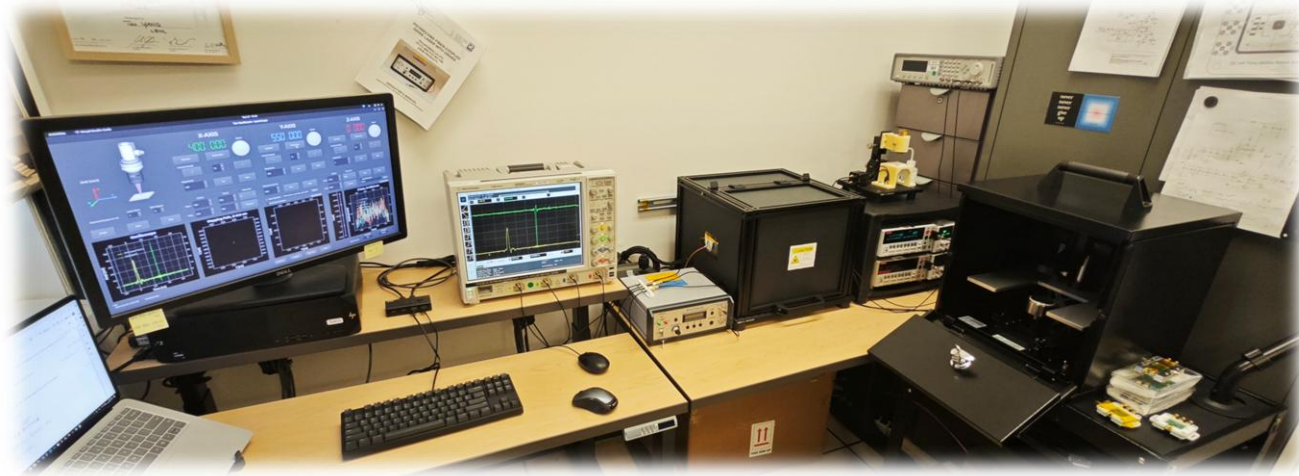
SiC Detector Test Setup of LBNL

Supported by LBNL Physics Division Detector R&D program (KA25)

- UV-TCT Setup



- SiC detector test workbench



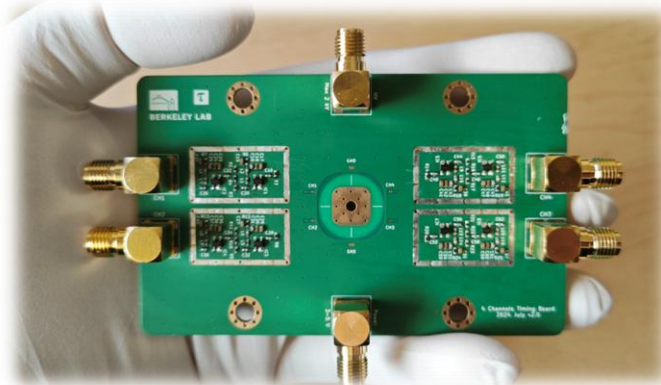
- HV probe station



- Single channel TIA board



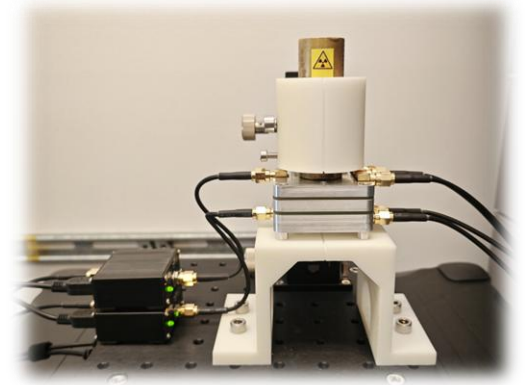
- Four channels TIA board



- α source test setup



- β source test setup



Contributions of Time Resolution by UV-TCT

$$\sigma_{TOT}^2 = \sigma_A^2 + \sigma_{Jitter}^2 + \sigma_{Trigger}^2 + \sigma_{TDC}^2 + \sigma_{sensor}^2$$

σ_A^2 is primarily dominated by time walk, which is mainly caused by variations in the energy deposition (such as laser energy consistency and the randomness of avalanche multiplication). This effect can be largely mitigated by using a Constant Fraction Discriminator (CFD).

σ_{Jitter}^2 is dominated by the signal-to-noise ratio (SNR), where $\sigma_{Jitter} = \frac{T_{Rise}}{SNR}$

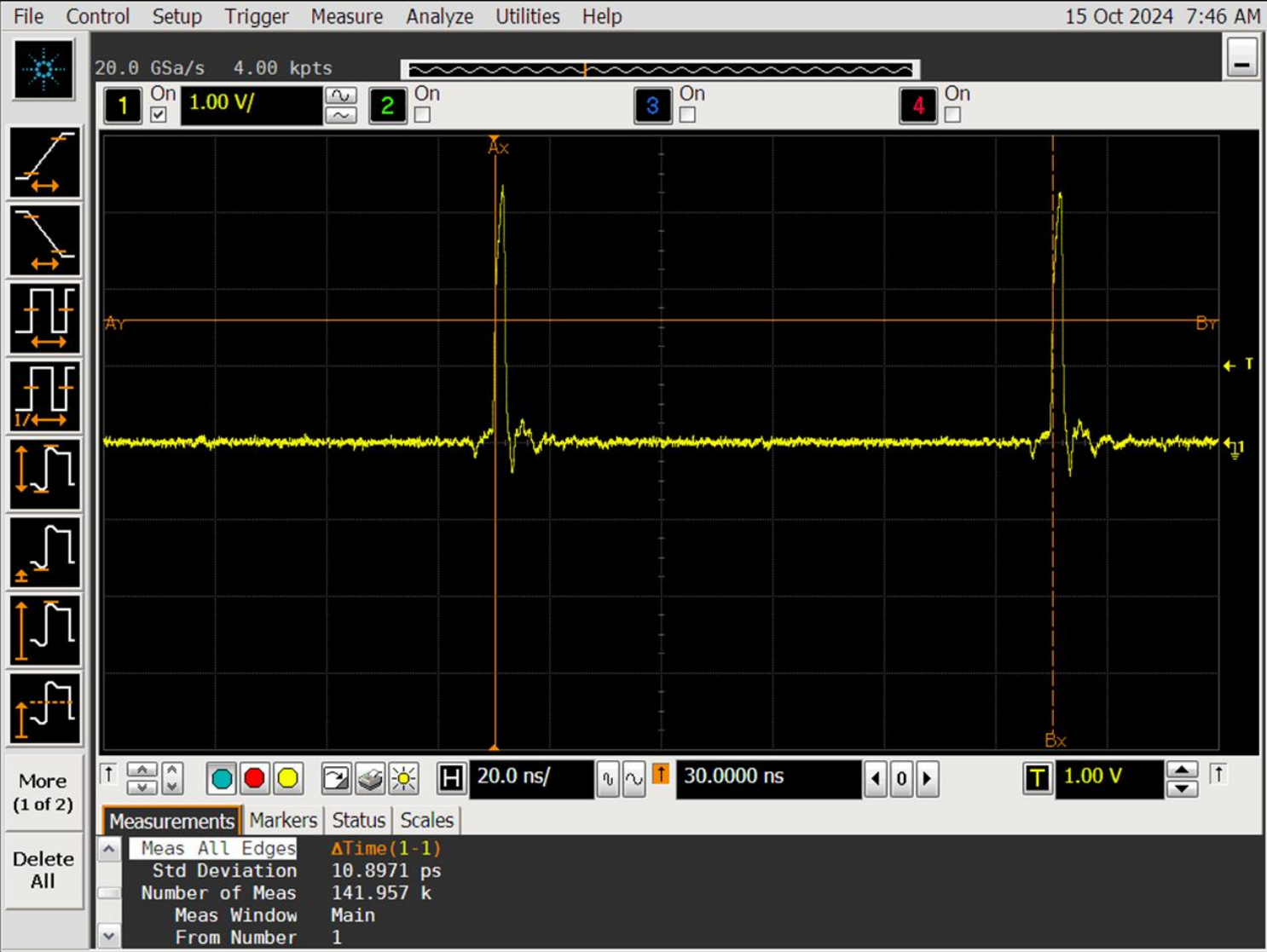
$\sigma_{Trigger}^2$ is dominated by laser sync trigger pulse which is constant. $\sigma_{Trigger} = 7.7 \text{ ps}$

σ_{TDC}^2 is dominated by sampling rate which is constant. For 20 GSa/s $\sigma_{TDC} = \frac{\Delta T}{\sqrt{12}} = 14.4 \text{ ps}$

σ_{sensor}^2 is dominated by electric field uniformity, device structure, ...

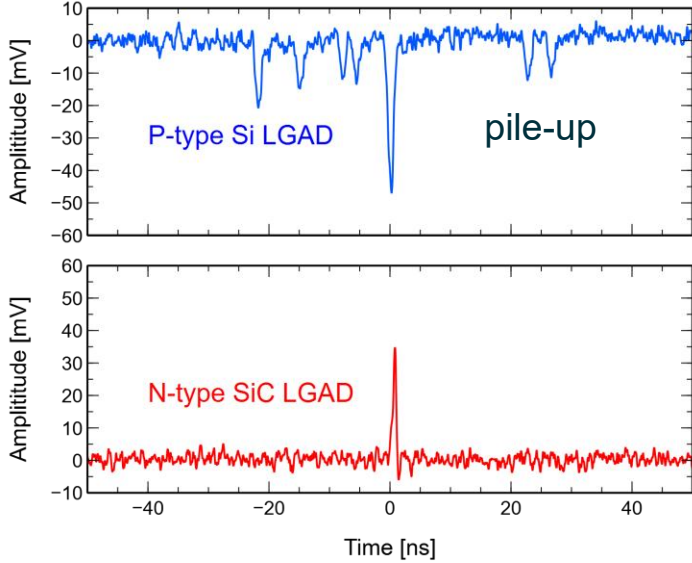
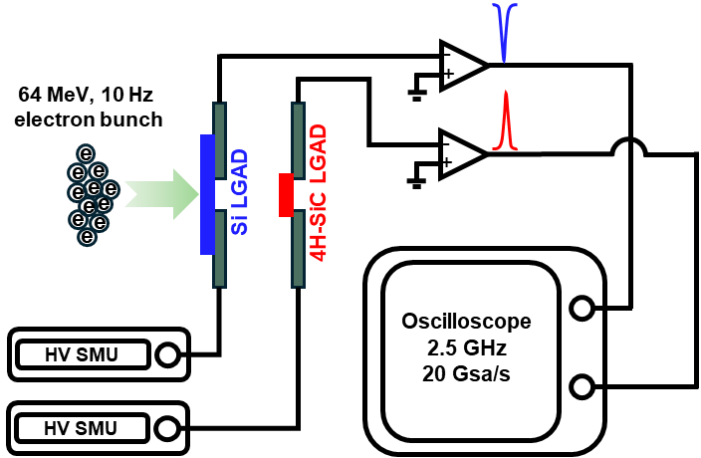
Laser sync trigger pulse

$$\sigma_{\text{Trigger}} = \sqrt{\frac{\sigma^2(T_{\text{post-pulse}} - T_{\text{pre-pulse}})}{2}} = 7.7 \text{ ps}$$



SLAC Beam Test

2025 April Run1



Beam energy:
64 MeV → 40 MeV



Beam rate:
10 Hz → 30 Hz

2025 July Run2

